

ISOFORM-SELECTIVE DISRUPTION OF AKAP-MEDIATED PKA  
LOCALIZATION USING HYDROCARBON STAPLED PEPTIDES

by

YUXIAO WANG

(Under the Direction of Eileen J. Kennedy)

ABSTRACT

A-kinase Anchoring Proteins (AKAPs) are key orchestrators that spatiotemporally regulate protein kinase A (PKA) activity by scaffolding pertinent intracellular proteins to form signaling complexes. Although PKA and AKAPs are involved in a variety of cellular and physiological functions, their exact roles in these functions and corresponding regulation mechanism are not well understood. In this thesis, several peptides mimicking the A-Kinase Binding (AKB) helix of AKAPs were chemically stabilized using all-hydrocarbon stapling, in order to target the docking/dimerization domain of PKA-R in an isoform-selective manner. The peptides are cell permeable in diverse human cell lines, highly isoform-selective for PKA-RI or -RII, and can effectively inhibit interactions between AKAPs and PKA-R in intact cells. Therefore, these peptides can be applied as valuable reagents in cell-based experiments to selectively disrupt AKAP-localized PKA-RI or -RII anchoring and aid in the study of compartmentalized type I or type II PKA signaling in cells.

INDEX WORDS: protein kinase A, A-kinase anchoring protein, all-hydrocarbon staple, peptide, fluorescence polarization, ring-closing metathesis

ISOFORM-SELECTIVE DISRUPTION OF AKAP-MEDIATED PKA  
LOCALIZATION USING HYDROCARBON STAPLED PEPTIDES

by

YUXIAO WANG

B.S., China Pharmaceutical University, China, 2011

A Thesis Submitted to the Graduate Faculty of The University of Georgia in  
Partial Fulfillment of the Requirements for the Degree

MASTER OF SCIENCES

ATHENS, GEORGIA

2014

© 2014

YUXIAO WANG

All Rights Reserved

ISOFORM-SELECTIVE DISRUPTION OF AKAP-MEDIATED PKA  
LOCALIZATION USING HYDROCARBON STAPLED PEPTIDES

by

YUXIAO WANG

Major Professor: Eileen J. Kennedy

Committee: Anthony C. Capomaccia

Yujun G. Zheng

Electronic Version Approved:

Julie Coffield  
Interim Dean of the Graduate School  
The University of Georgia  
August 2014

## DEDICATION

To my parents and my fiancé  
For their support, love and belief in me.

## ACKNOWLEDGEMENTS

First of all I would like to thank my major professor and my mentor, Dr. Kennedy, for her guidance since I joined this lab. Nothing I achieved here at UGA would have been possible without her assistance, support and encouragement.

I would also like to thank Dr. Capomacchia and Dr. Zheng for serving on my committee and for their valuable suggestions.

I thank Dr. Beedle for her patient and kind help on many technical issues in the lab. I am also grateful to Dr. Momany, who brought me into this department.

My deepest appreciation goes to my friends and lab mates Laura Hanold, Sneha Patel, Melody Fulton, Grace Ho, Lewis Schendowich, Avinash Sukhu, Weihao Zhang, Xin Li and my fiancé Runqing Diao, for their care, support, advice and love.

## TABLE OF CONTENTS

	Page
ACKNOWLEDGEMENTS .....	v
LIST OF TABLES.....	viii
LIST OF FIGURES.....	ix
CHAPTER	
1 INTRODUCTION AND LITERATURE REVIEW .....	1
PROTEIN KINASE A.....	1
A-KINASE ANCHORING PROTEIN.....	7
DISRUPTION OF PKA-AKAP USING HYDROCARBON STAPLED PEPTIDES.....	14
2 RII-SELECTIVE DISRUPTION OF AKAP-LOCALIZED PKA USING HYDROCARBON STAPLED PEPTIDES .....	25
ABSTRACT .....	26
INTRODUCTION .....	27
RESULTS AND DISCUSSION.....	29
CONCLUSION.....	35
METHODS.....	36
3 DISRUPTION OF AKAP-MEDIATED TYPE I PKA LOCALIZATION USING HYDROCARBON STAPLED PEPTIDES.....	57
ABSTRACT .....	58

INTRODUCTION .....	59
RESULTS .....	61
DISCUSSION .....	68
METHODS.....	70
4 SUMMARY.....	89
REFERENCES.....	91

## LIST OF TABLES

	Page
Table 1.1: Sequence of AKB sequences used as templates .....	23
Table 3.1: $K_D$ of STRIAD peptides binding full-length R subunits .....	82

## LIST OF FIGURES

	Page
Figure 1.1: Domain organization of PKA-R subunits .....	18
Figure 1.2: AKAP-mediated signaling complex.....	19
Figure 1.3: Amphipathic helical A-kinase binding domain of AKAP .....	20
Figure 1.4: Comparison of RII $\alpha$ D/D and RI $\alpha$ D/D.....	21
Figure 1.5: Isoform-specific disruption of PKA signaling.....	22
Figure 1.6: Targeting R subunits using hydrocarbon stapled peptides .....	24
Figure 2.1: Sequences for design of stapled peptides .....	44
Figure 2.2: Parent sequence peptides did not gain intracellular access.....	45
Figure 2.3: Screening of Lys modified library using R D/D .....	46
Figure 2.4: Fluorescence polarization of 1K library of peptides .....	47
Figure 2.5: Fluorescence polarization of 2K library of peptides .....	48
Figure 2.6: Fluorescence polarization of 3K library of peptides .....	49
Figure 2.7: Stapled peptides are highly selective for PKA-RII .....	50
Figure 2.8: Hydrocarbon staple significantly increases cell uptake .....	51
Figure 2.9: Cell permeability of STAD scramble control peptides.....	52
Figure 2.10: STAD peptides can target RII in cells .....	53
Figure 2.11: STAD peptides can effectively block PKA signaling in cells .....	54
Figure 2.12: STAD peptides affect only anchored PKA activity .....	55
Figure 2.13: PKA response in cells without peptide treatment .....	56

Figure 3.1: Alignment of several RI- and RII-specific AKAP sequences.....	76
Figure 3.2: Targeting RI D/D using hydrocarbon stapled peptides .....	77
Figure 3.3: PKA-R D/D binding of hydrocarbon stapled peptides .....	78
Figure 3.4: Binding curves of hydrocarbon-stapled peptides on R D/D .....	79
Figure 3.5: Insufficient uptake of wt and v1 .....	80
Figure 3.6: Helical wheel presentation of RIAD sequence.....	81
Figure 3.7: Binding curves of STRIAD peptides on full-length R subunits.....	83
Figure 3.8: Ht31 competition assay .....	84
Figure 3.9: Ht31PP competition assay as control .....	85
Figure 3.10: Effective uptake of STRIAD peptides by MDA-MB-231 cells.....	86
Figure 3.11: Effective uptake of STRIAD peptides by PC-3 cells .....	87
Figure 3.12: STRIAD peptides selectively target RI in cells.....	88

## CHAPTER 1

### INTRODUCTION AND LITERATURE REVIEW

#### PROTEIN KINASE A

Protein kinase A (PKA) or cAMP-dependent protein kinase, is a broad specificity kinase that requires concerted spatiotemporal regulation to exert its diverse cellular functions[1]. Binding of ligands such as hormones or neurotransmitters onto G-protein coupled receptors (GPCRs) promotes adenylyl cyclase (AC) to synthesize cAMP, which in turn activates PKA. The PKA holoenzyme is a tetramer consisting of two catalytic subunits and two regulatory subunits. When inactive, the active sites of catalytic subunits are covered by the pseudosubstrate region of regulatory subunits. Upon the binding of two cAMP molecules onto each regulatory subunit, the two catalytic subunits are released and become available to phosphorylate substrates within their proximity[2]. Isoforms of regulatory subunits of PKA can be divided into two general classes, RI and RII. Historically, the catalytic subunits isolated from type I and type II PKA are functionally and structurally the same, while the regulatory subunits are much more different from an immunological aspect and in primary structure[3]. Therefore, the holoenzyme complex consists of catalytic subunits and RI or RII subunit is referred as type I or type II PKA. Although there are three isoforms ( $\alpha$ ,  $\beta$ ,  $\gamma$ ) of catalytic subunits discovered, none of them have shown preference to RI

or RII in terms of co-expression[4]. Cloning of cDNA for the regulatory subunits has identified four isoforms: RI $\alpha$ , RI $\beta$ , RII $\alpha$  and RII $\beta$ . Although these four isoforms share a common domain organization based on extensive sequence similarity, they are functionally non-redundant. In particular, the overall architecture of these isoforms seems to be quite distinct. Domains of the isoforms also have various functions that contribute to protein-protein interactions in unique ways and thereby to the general signaling network[5].

Overall, all regulatory isoforms share similar general organization of functional domains, which contain two tandem cAMP-binding domains (CBD) at C-terminus and a variable segment (including D/D domain and peptide inhibitory site) at N-terminus[6] (Figure 1.1). The two tandem cAMP-binding domains encompass two thirds of the protein[7] and are highly conserved in both RI and RII. However, the N-terminus of the two isoforms differs significantly in many regions. In fact, most antibodies are able to distinguish regulatory subunit isoforms due to the sequence variability in this region. In addition, the hinge region is important for the interaction between regulatory subunit and catalytic subunit in both RI and RII. In RII, the proteolytic-sensitive hinge region that occupies the catalytic domain of the C subunit contains a Ser95 as an autophosphorylation site, while the corresponding residue of RI is replaced with a Gly/Ala, which serves as an unphosphorylatable pseudosubstrate site[7-9] (Figure 1.1). Autophosphorylation of Ser95 in RII subunit reduces the affinity to the catalytic subunit by almost 10-fold[10]. Since the phosphorylated RII has a reduced affinity for the catalytic subunit, it dissociates at a lower concentration of

cAMP as compared to the dephosphorylated RII. When the type II holoenzyme complex dissociates, the phospho-Serine becomes more accessible to phosphatases and can be dephosphorylated. The linker region next to the stable domain are very mobile and variable[11]. The N-linker hinge region itself is also a substrate of several other protein kinases. Phosphorylation of this region seems to have an effect on the interaction between regulatory subunits and other proteins including AKAPs. The stable N-terminal region is referred to as the docking/dimerization (D/D) domain, because it is formed from two regulatory subunits to create a groove surface that can be targeted by AKAPs. The overall structure and folding of RI D/D and RII D/D is similar, they are both made of an antiparallel X-type four-helix bundle[12, 13], but also differ in several ways that have been highlighted by X-ray crystallography studies[14, 15]. These similarities and differences will be further discussed in the following section.

Before high-resolution structures of the  $R_2$  homodimer or R-C complex were solved, small-angle X-ray scattering (SAXS) and small-angle neutron scattering (SANS) prevailed as methods to investigate the quaternary assembly of the R subunit homodimers, R-C heterodimers and even  $R_2C_2$  tetramers. Several SAXS studies showed that structures of both  $R_{II\alpha}$  and  $R_{II\beta}$  homodimers have extended, flexible, rod-like shapes, while the  $R_{I\alpha}$  homodimer has a well-defined Y-shape structure that is more compact and shorter than the RII homodimers[16].  $R_{I\beta}$  homodimers have similar overall compact shapes with  $R_{I\alpha}$  in the absence of C subunits, but the two isoforms differ significantly when assembled into a tetramer with the C subunits[17].  $R_{I\alpha_2}C_2$  has a compact V-

shape while  $R\text{I}\beta_2\text{C}_2$  has an extended cylinder-like shape. Similarly, although  $\text{RI}\alpha$  and  $\text{RII}\beta$  subunits show similar overall shapes as homodimers, they differ markedly when forming a complex with the C subunit.  $\text{RII}\beta_2\text{C}_2$  is compressed to form a globular shape upon from  $\text{RII}\beta_2$  dimer while  $\text{RII}\alpha_2\text{C}_2$  complex remains in an extended dumbbell shape in the holoenzyme complex[18]. Therefore, SAXS/SANS data have shown that the quaternary shapes of all four isoforms holoenzyme complex are different despite their extensive homology in primary sequence. In the past 10 years, multiple high-resolution crystal structures of different mutant R isoforms in RC or  $\text{R}_2\text{C}_2$  complex have been resolved, providing substantial structural insights into the tetrameric assembly and conformational change upon cAMP activation[17, 19-25]. This result is consistent with the fact that  $\text{R}_2\text{C}_2$  complex of different isoforms have distinct tetrameric interfaces and isoform-specific quaternary structures while the structures of heterodimers are similar and have a two-fold axis of symmetry for the different R isoforms. These differences in structures shed light on the mechanism of R-C docking as well as the non-redundant biological functions of the regulatory subunit isoforms. Recently, crystal structures of both  $\text{RI}\alpha$  and  $\text{RII}\beta$  bound to cAMP were solved using R-subunit constructs containing only the inhibitor site and cAMP-binding domains, providing more insight into isoform-selective cAMP analogs activation[26].

RI and RII vary in their expression levels in different tissues[27].  $\text{RI}\alpha$  is ubiquitously expressed in most tissues, while  $\text{RI}\beta$  is expressed primarily in brain, testis, and B and T lymphocytes.  $\text{RII}\alpha$  is also ubiquitous in its distribution,

whereas RII $\beta$  is found mainly in brain, adipose, and some endocrine tissues[28]. Additionally, the relative amount of RI and RII also varies in phases of the cell cycle and other physiological conditions[29], suggesting that the two types of regulatory subunits have distinct roles in different cellular processes. PKA, as a broad specificity kinase, is known to be involved in a variety of cellular processes like energy metabolism, DNA replication, cell division, cell proliferation and cell death[30]. It's not surprising that it contributes to various disease states like diabetes, neurodegenerative diseases, airway diseases, cardiovascular diseases and cancer. Traditionally, RII is the isoform that directs the C subunits to target compartments in most of the reported PKA-mediated signaling events, while the role of RI is more elusive. It's suggested that one of RI's role is to act as a universal buffer against unregulated C subunits[31]. When the C subunit is overexpressed in cell culture, a compensational phenomenon to keep the R: C ratio at 1 was observed through overexpression of RI $\alpha$  but not RII $\alpha$  subunit[32]. In another set of experiments, overexpression of RII in NIH 3T3 mouse fibroblasts completely eliminated the formation of the type I complex, while overexpression of RI did not affect the formation of type II complex, suggesting that the assembly of PKA holoenzyme complex favors RII over RI[33]. Similar compensation effects by RI $\alpha$  were observed *in vivo* in RI $\beta$  or RII $\beta$  knock-out mice[34, 35]. However, some deficits in phenotypes were still observed even though overexpressed RI $\alpha$  managed to retain the R: C ratio at 1, suggesting non-redundant roles between these R isoforms. Surprisingly, RII $\alpha$  knockout mice are viable, fertile and did not show any obvious phenotype[36, 37]. RII $\beta$  knockout

mice are also viable, lean and resistant to diet-induced obesity[38]. In contrast to the moderate outcomes of other isoforms, knocking out RI $\alpha$  in mouse led to embryonic lethality[39]. RI $\alpha$ 's exclusive compensation ability might explain the drastically different phenotypic consequences of knocking out RI $\alpha$  versus other R isoforms. Even though buffering the unregulated catalytic subunit seems to be an important role of RI, it's definitely not the only function it exerts in the cell. This is supported by increasing numbers of studies showing RI can be localized to particular subcellular compartments like RII. For example, an *in vivo* study suggests RI is localized to the neuromuscular junction in skeletal muscle, and appears to regulate L-type Ca<sup>2+</sup> channels[36, 40]. Another example includes the localization of RI to activated TCR complexes in human T lymphocytes[41]. The Carney complex is the first human disease mapped to PKA R subunit[42]. Familial cases mapping of this disease reveals deletions/mutations in the RI $\alpha$  coding exons leading to frame shifts and premature stop codons. It's been concluded that that loss of RI $\alpha$  in Carney complex patients leads to dysregulated PKA activity, increased responsiveness to cAMP, and excess of type-II PKA activity[31]. Accumulating discoveries of RI-specific AKAPs also suggest that type I PKA does have a non-redundant role in cellular localization and corresponding functions.

PKA, as a prototype of protein kinases, has received continuous attention over forty years since its initial discovery. People's understanding on this broad-specificity signaling kinase has been deepening as more and more interest is focused on this field. However, the exact mechanism of regulation of PKA

activity, especially its fascinating capacity to discretely regulate various signaling pathways at a global level, is still unclear. Recognition of the interaction between RI/RII and AKAP has introduced us into a whole new field of spatiotemporal regulation.

## **A-KINASE ANCHORING PROTEINS**

A-kinase anchoring proteins (AKAPs) are a diverse scaffolding protein family that targets PKA to distinct compartments of the cell[43]. Up to date, over 50 different AKAPs are have been identified[44]. AKAPs anchor PKA to various subcellular environments mainly through an  $\alpha$ -helix named AKB (A-kinase binding domain), which binds the D/D (docking/dimerization) domain formed by PKA regulatory subunit dimer[45]. The interaction between the AKB helix and D/D domain is predominantly driven by hydrophobic interactions, as shown by several structural studies on amphipathic helical AKB peptides and the D/D domain of both regulatory subunit isoforms[13-15]. Besides PKA, AKAPs also associate with other protein kinases, phosphatases, phosphodiesterases and potential substrates of these enzymes, forming a signaling complex with intrinsic specificity among the relevant interacting partners[44] (Figure 1.2). Therefore, AKAP-mediated localization through the R subunits is very important for the spatiotemporal regulation of PKA signaling. To date, most identified AKAPs favor binding to the RII isoform, covering diverse physiological and pathological functions including sperm function, oocyte formation, embryogenesis, memory, cardiac function and cancers. Only a few AKAPs have proven to be RI-specific,

including SKIP[46] in the cytoplasm and small membrane AKAP[47] which is enriched at the cell membrane. There are also several AKAPs like D-AKAP1 and D-AKAP2 that are dual specific, meaning they can bind to both RI and RII with appreciable affinity. Most AKAP-RII complexes are directed to specific subcellular compartments while AKAP-RI complexes tend to diffuse in the cytoplasm, although exceptions have been reported[47].

Members of the AKAP family are structurally and functionally diverse, while they are grouped together because of the shared ability to anchor PKA, mostly through the interaction with the amphipathic AKB helix [48]. Therefore, this section will be mainly focused on this particular. In 1989, a mapping study of microtubule-associated protein 2 (MAP2) identified a primary sequence of 20 amino acids that interacts with PKA, which is displayed as an amphipathic helical conformation via helical wheel analysis[48, 49]. Ever since this first-identified AKAP, people realized that the arrangement of hydrophobic and hydrophilic residues on the opposite side of the helix is a conserved, defining characteristic of the AKB domain for the majority of members within the AKAP family[50] (Figure 1.3b). A number of biochemical and functional studies performed have confirmed this, in line with the first direct structural data of the helical AKB peptides by 3D NMR, where Newlon et al. presented two complexes formed by RII $\alpha$  D/D and AKAP peptides (Ht31-RII and AKAP79-RII)[13]. The RII $\alpha$  D/D domain in these complexes shows that the dimer forms an X-type four-helix bundle with the two protomers adopting an antiparallel conformation, while the AKAP helix (Ht31 and AKAP79) binds in the hydrophobic groove at 50° angle

across the dimer interface. This study further confirmed, even though there was minimal sequence conservation, that the AKB of AKAPs shares a conserved helical amphipathic motif, with the hydrophobic surface docking into the hydrophobic groove that was preformed by the N-terminal helices from both RII $\alpha$  protomers. The high-resolution crystal structure of the RII-AKAP-IS (a RII-specific peptide designed in silico) complex was obtained by Gold in 2006 [51]. Overlay of this structure onto the apo RII did not show much difference, revealing that RII has a rigid docking surface for AKAPs. Parallel with this study, another high resolution crystal structure of RII-AKAP complex was submitted at the same time[14]. The AKAP peptide used in this study is a RII-specific peptide derived from AKB of D-AKAP2, but the two RII D/D structures superimposed very closely to each other. One difference proposed by the second crystal structure is that N-terminus of one protomer of RII $\alpha$  D/D is tightly bound to the AKAP peptide whilst the second promoter is disordered. This dynamics introduced by the disordered N-terminus may partly explain why RII is so accommodating and tolerant to different AKAP sequences. Despite the fact that most AKAPs bind RII with much higher affinity than RI, this structure confirmed a feature of AKB that's known to favor RI binding over RII. This structural feature requires having a bulky side chain at position 13 (or corresponding position in other sequences), because there is a cavity in the RI D/D to accept the bulky side chains. In contrast, RII D/D cannot accommodate aromatic residues at position 13 and has a strong preference for Val over Trp due to the absence of such a cavity.

Although the initial identification of AKAPs is solely through RII interactions, the discovery of dual-specific AKAPs[52] and several RI-specific AKAPs[53, 54] gave an impetus to solve the structure information of the RI regulatory D/D, which found both the similarities and differences between RI D/D and RII D/D[12, 55]. The overall structure of the RI $\alpha$  D/D is similar to RII $\alpha$  D/D, an X-type four-helix bundle. They both include a turn separating two conserved helical regions, one involves PKA docking and the other plays a role in dimerization. One of the major differences that stood out is the distinct AKAP-PKA R contact interface. On the contrary to the shallow groove formed by the surface of RII D/D dimer, the RI D/D forms a much deeper cleft, which might explain why RI D/D is more discriminating in terms of AKB sequence of AKAPs (Figure 1.4). Another difference is the existence of two unusual inter-chain disulfide bonds in RI $\alpha$  D/D (Figure 1.4), forming a somewhat more compact docking module in contrast to the non-covalent dimer of RII D/D. Additionally, RI $\alpha$  contains several acidic and basic residues at the docking groove, as compared to the mostly hydrophobic interface of RII $\alpha$ [12]. Dual-specific AKAP2 (D-AKAP2) binds both RI and RII D/D at nanomolar range, which has made this particular AKAP under intensive study to identify the mechanism of isoform selectivity of AKAPs. Burns-Hamuro et al. utilized Hydrogen/deuterium (H/D) exchange combined with mass spectrometry (DXMS) to probe backbone structural changes of the AKB domain from D-AKAP2 docked to both RI and RII D/D[45]. Their results showed that RI D/D has an increased helical stabilization of the docked AKB ligand as compared to RII D/D, suggesting that RI $\alpha$  D/D has more binding

constraints for the AKB ligand in the binding state. On the contrary, that of RII D/D was shown to have a preformed and local binding surface. All the guessing and extrapolation about RI-AKAP interactions have finally found a solid foundation when the high resolution crystal structure of RI-AKAP complex was resolved in 2010[15]. The new structure agreed with the existence of inter-chain disulfide bonds, and indicated that these two disulfide bonds are involved in AKAP anchoring. RMSDs obtained from this complex structure and RI D/D apo structure indicated a rearrangement of the two monomers upon binding of the AKAP peptides. The AKAP peptide binds diagonally onto the hydrophobic groove of RI $\alpha$  D/D, which is similar as its binding in RII $\alpha$  D/D[14]. In contrast to RII $\alpha$  D/D, the N-terminal region of both monomers are ordered and form structurally similar helices. Additionally, an unexpected difference is the shift in the  $\alpha$ -helical register by a complete turn. Based on this observation and other spatial restrictions by the residues lining the pockets, the authors proposed several specific requirements for binding to R isoforms in each of the four hydrophobic pockets (See reference 15). The RI-AKAP and RII-AKAP crystal structures thus provided invaluable insight into the isoform specific binding mechanism of PKA RI and RII, which laid the powerful foundation for developing isoform-specific AKAP mimicking disruptors.

Although AKAP family has been implicated to be functionally diverse, the shared cellular role of most AKAPs is to anchor all relevant protein kinases, protein phosphatases, phosphodiesterases and other substrates or effectors into proximity and into a preferred orientation, allowing the spatial and temporal

regulation of particular signaling pathways[30]. This mode of regulation is the molecular basis of confining a global signaling modulator's activity like PKA. The exact biological relevance of individual AKAPs has been extensively studied by various means such as gene knock-outs, RNAi and peptide disruptors. L-type  $\text{Ca}^{2+}$  channels have been studied intensively in the context of AKAPs and proved to be involved with numerous AKAPs, such as AKAP79, mAKAP and AKAP15/18, in several different types of cells[56-58]. Another well-studied example is the involvement of AKAP18 $\delta$  in  $\text{Ca}^{2+}$  reuptake to sarcoplasmic reticulum[59]. siRNA knockdown experiments suggested that the AKAP18 $\delta$ -facilitated complex enabled the finely tuned control of PKA phosphorylation on phospholamban, which regulates on  $\text{Ca}^{2+}$  reuptake into sarcoplasmic reticulum through sarcoplasmic reticulum  $\text{Ca}^{2+}$ -ATPase 2 (SERCA2). More than 50 different AKAPs have been identified with wide-spectrum tissue distribution and cellular functions that I will not be able to describe thoroughly[60].

Being a key spatiotemporal regulator of PKA, AKAPs also have been implicated in playing essential roles in wide range of both physiological and pathological processes, such as endocrinological, nephrological, neurodegenerative, cardiovascular and immune diseases and multiple types of cancer[61]. The pathological conditions in most reported studies are associated with only dysregulation or malfunction of specific AKAPs but not a global PKA/cAMP signaling change, highlighting the importance of the PKA subcellular localization by AKAP. The most studied AKAP-related pathophysiology is cardiac diseases, where multiple AKAPs are involved with a variety of processes,

through regulation of different PKA phosphorylation substrates such as L-type  $\text{Ca}^{2+}$  channels, type 2 ryanodine receptors (RyR2) and phospholamban[61]. Overall, phosphorylation of these substrates leads to  $\text{Ca}^{2+}$  fluxes and thereby enhancement of contractility. Genetic polymorphisms, gene knockouts and dysregulations of AKAPs have resulted in altered phenotypes like long-QT syndrome[62], shortening of the PR interval of the cardiac cycle[63], elevated resting heart rate and diminished heart rate variability[64], and chronic heart failure[65], providing direct evidence for AKAPs' role in cardiac functions. AKAPs also have extensive involvement in both the male and female reproductive systems. Particularly, WAVE-1's role of anchoring PKA and the tyrosine kinase Abl to the nuclear envelope is well characterized in the process of oocyte maturation[66]. AKAP3 and AKAP4, on the other hand, play an important role in sperm motility[67]. Of increasing interest is the role of AKAP in cancer. Gravin, an AKAP expressed in many different tissues, has been recognized as a tumor suppressor, mainly due to its ability to induce cell cycle arrest and apoptosis in numerous cell types[68]. What really drew attentions to the concept of AKAP-mediated PKA compartmentalization in cancer is a single nucleotide polymorphism (SNP) that is located in the AKB domain of D-AKAP2. This SNP has been associated with cardiac dysfunction and higher risk of familial breast and colorectal cancer[63, 64, 69]. Additionally, SNPs in several other AKAPs can also lead to the development breast cancer[70, 71], indicating the profound implication of AKAP-mediated signaling in cancer development.

## **DISRUPTION OF PKA-AKAP USING HYDROCARBON STAPLED PEPTIDES**

Although more and more AKAP-mediated signaling pathways have been implicated in the etiology of various diseases, the precise model of these pathways and their mechanisms of regulation are not fully understood. Specifically, what are the proteins or factors in the AKAP signaling complex that are involved? How are PKA signaling events restrictively initiated and terminated? How are the signaling cascades regulated? How does malfunction of the proteins or dysregulation of signaling eventually lead to the phenotype of diseases? In order to uncover the relevance of AKAPs in physiological and pathological processes, a plethora of questions like these needs to be answered in a disease-specific context. Taking the previously mentioned SNP mapped in the A kinase binding domain of D-AKAP2 as an example, it was identified as a disease susceptible mutation as it's associated with cardiac dysfunction, familial breast cancer and colorectal cancer[63, 69, 72]. This SNP of D-AKAP2 caused three-fold increase of binding affinity to RI but not RII, in line with the alteration of subcellular localization of type I but not type II PKA. Given the fact that overexpression of RI over RII has been documented as hallmark of various cancers, it is proposed that altered D-AKAP2-mediated compartmentalization of type I PKA contributes to the associated pathological effects through misregulation of downstream type I-specific PKA substrates phosphorylation. However, no specific PKA signaling pathways are associated with D-AKAP2, nor have any PKA substrates that are specifically linked to D-AKAP2 are identified. These pieces of unknown knowledge are the key basis for elucidating the

biological role of D-AKAP2, RI/RII and isoform-specific signaling regulation in cardiac diseases and cancers, which is in great demand due to the lack of novel and effective therapeutic strategies.

To address such needs, isoform-selective disruption of interactions between PKA-R and AKAPs using novel chemical or biological agents has received more and more attention (Figure 1.5). A promising class of candidates in disrupting protein-protein interactions is peptide or peptidomimetics. Indeed, a tremendous amount of work have been done to develop peptides mimicking the AKB of AKAPs as a strategy to target AKAP-PKA interactions[73]. A more detailed review of these peptides will be discussed in the **Introduction** Section of **Chapter 2** and **Chapter 3**. Although these peptides have shown high specificity in blocking RI- or RII-mediated PKA-AKAP interactions, they are limited by the intrinsic disadvantages of peptides, including loss of secondary structure, inability to permeate cell membranes and proteolytic instability. Therefore, we propose to apply a chemical-stabilizing modification method called all-hydrocarbon stapling to these peptides in order to improve the biophysical properties of the peptides. This method combines two individual helical stabilization strategies,  $\alpha$ ,  $\alpha$ -disubstitution and macrocyclization. Through enhanced  $\alpha$ -helical content by this method, introduction of a hydrocarbon staple has been proven in numerous studies to achieve enhanced pharmacological properties such as increased target affinity, improved cell uptake by the endocytic pathway, higher resistance to proteolytic degradation and longer *in vivo* half-lives (multiple studies reviewed in [74]). More importantly, the modification will preserve the interface between

AKB and D/D domain and hence does not impair binding to the PKA R subunit. As bioactivity and bioavailability are optimized, these peptides represent a new strategy to target intracellular protein-protein interactions and are invaluable tools to study AKAP-mediated signaling pathway *in cellulo* and *in vivo*, and may also act as potentially novel clinical agents to target AKAP-related diseases.

Based on isoform specificity of the regulatory subunits, AKAPs can be divided into three different categories: RI-, RII- and dual-specific. Extensive studies have delineated the relationship between the primary sequence of the PKA regulatory binding (AKB) domain and isoform-specificity[75, 76]. Crystal structures of the  $\alpha$ -helical AKB of AKAPs diagonally binding across the surface of RI or RII docking/dimerization (D/D) domain have been resolved, shedding light on sequence design of AKAP mimicking peptides[14, 15]. Additionally, rational design and point mutations based on natural AKB sequences gave rise to artificial peptide sequences with isoform-specific nanomolar binding affinities[51, 75, 77, 78]. With solid groundwork available, AKAPs with high affinity and specificity to RI or RII are valuable templates for the development of peptide disruptors[46, 47, 79]. We aimed to keep the hydrophobic patch of the  $\alpha$ -helical template peptide intact so as to preserve the interaction with PKA-R D/D domain, while introducing the helix-stabilizing hydrocarbon staple onto the backside of helix. Theoretically, stapled RI and RII peptide disruptors can be synthesized by using different AKAP sequences as templates.

To start off, seven AKB sequences were chosen as templates to design hydrocarbon stapled peptides (Table 1.1). All of these peptides share the

common feature of appropriately spaced hydrophobic registers that are indispensable for binding the PKA regulatory subunits, leaving those residues on the opposite side of the  $\alpha$ -helix available for chemical modification. To embed the hydrocarbon staple, a pair of nonessential residues at  $i$  and  $i+4$  position will be substituted by the  $\alpha$ -methyl,  $\alpha$ -alkenyl amino acids known as S5 (Figure 1.6). The hydrophobic residues required for binding will be excluded from modifications.. The two alkenyl chains will be cross-linked together through olefin metathesis using Grubb's catalyst. Techniques to synthesize hydrocarbon stapled peptides have been fully developed and systematically described[80]. Multiple sites for insertion of hydrocarbon staple will be chosen for each parent sequences. Therefore, variants with staples at different position will be derived from each parent sequences, generating the initial library to be screened in the following characterization experiments. Modification of the template sequences might be performed as the progress of optimization. Knowledge we gain from these assays can provide feedback for us to further optimize until desired properties are accomplished. The progress of screening, optimization, development and validation for RI- and RII- selective disruptors will be discussed in **Chapter 2** and **3**, respectively.

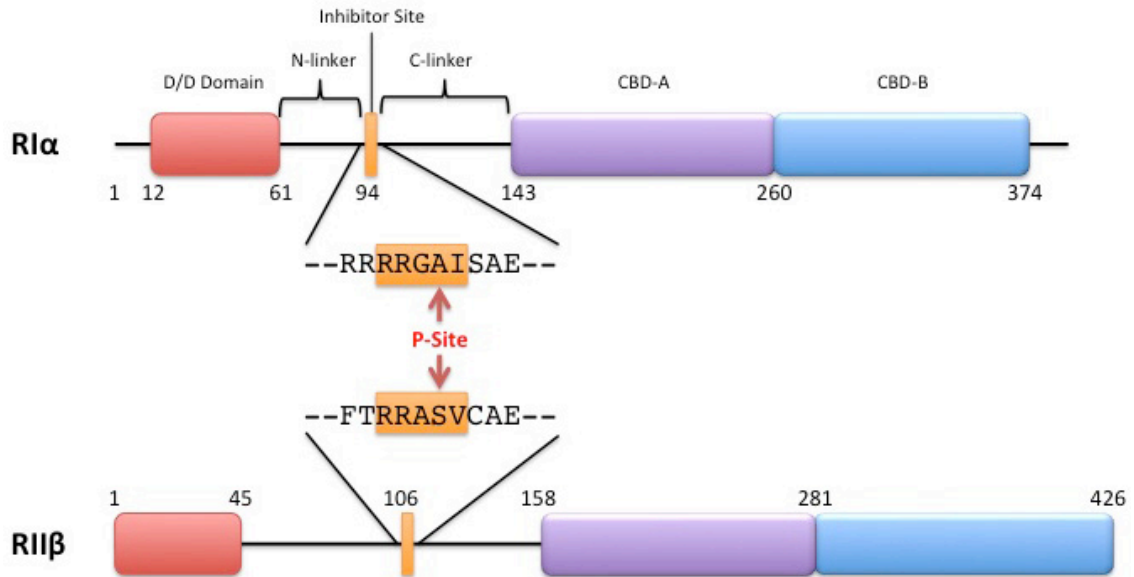


**Figure 1.1 Domain organization of PKA-R subunits.** Cartoon presentation of the domain organization for R1 $\alpha$  and RII $\beta$ . Docking/dimerization (D/D) domains are shown as red boxes. Inhibitor sites are shown as yellow boxes. Cyclic nucleotide binding domains (CBD) A and B are shown as purple and blue boxes, respectively. Phosphorylation sites are marked by red arrow.

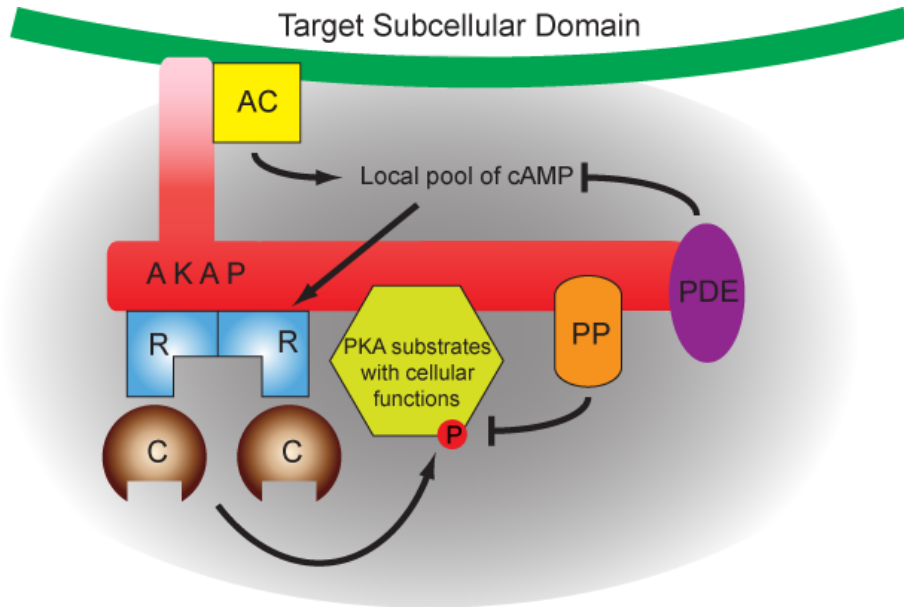


**Figure 1.2 AKAP-mediated signaling complex.** AKAPs regulate the phosphorylation of PKA substrates in a spatiotemporal manner by recruiting related machinery to subcellular locations for compartmentalized signaling.

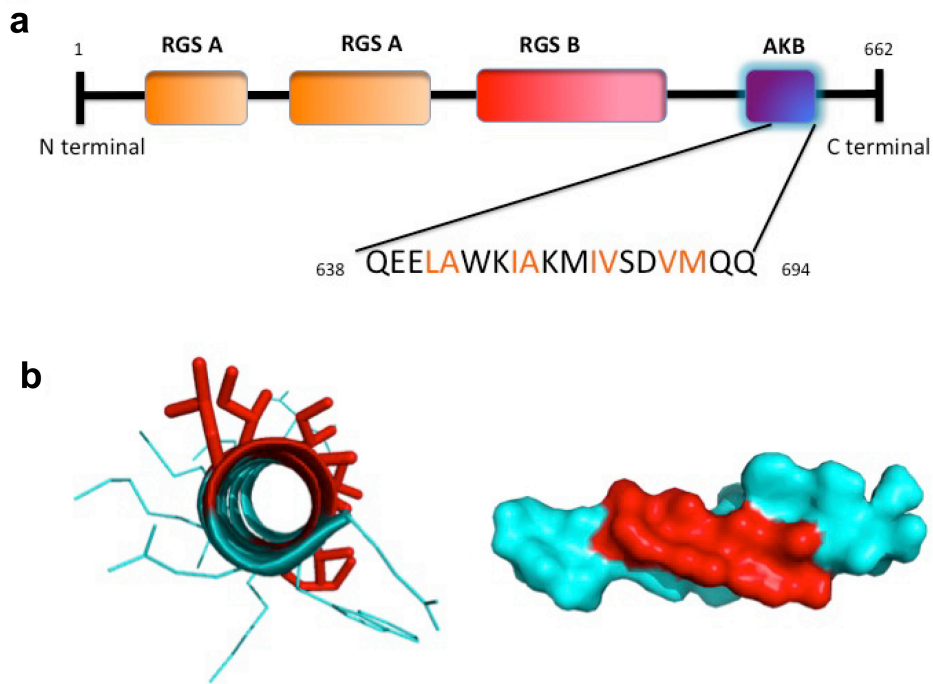


**Figure 1.3 Amphipathic helical A-kinase binding (AKB) domain of AKAP.**

(a) Domain representation the primary sequence of AKB domain of an AKAP member called D-AKAP2. Hydrophobic residues are shown in red. (b) The crystal structure of the helical AKB peptide from panel (a), showing the hydrophobic patch forming at one side of the helix. On the left, the backbone of AKB is shown in cartoon format and the side chains are shown as sticks. On the right, the entire AKB is shown as spheres. In both images, hydrophobic residues are colored in red. The images are modified based on structures from Sarma. et al., 2010 (PDB: 3IM4) using Pymol.

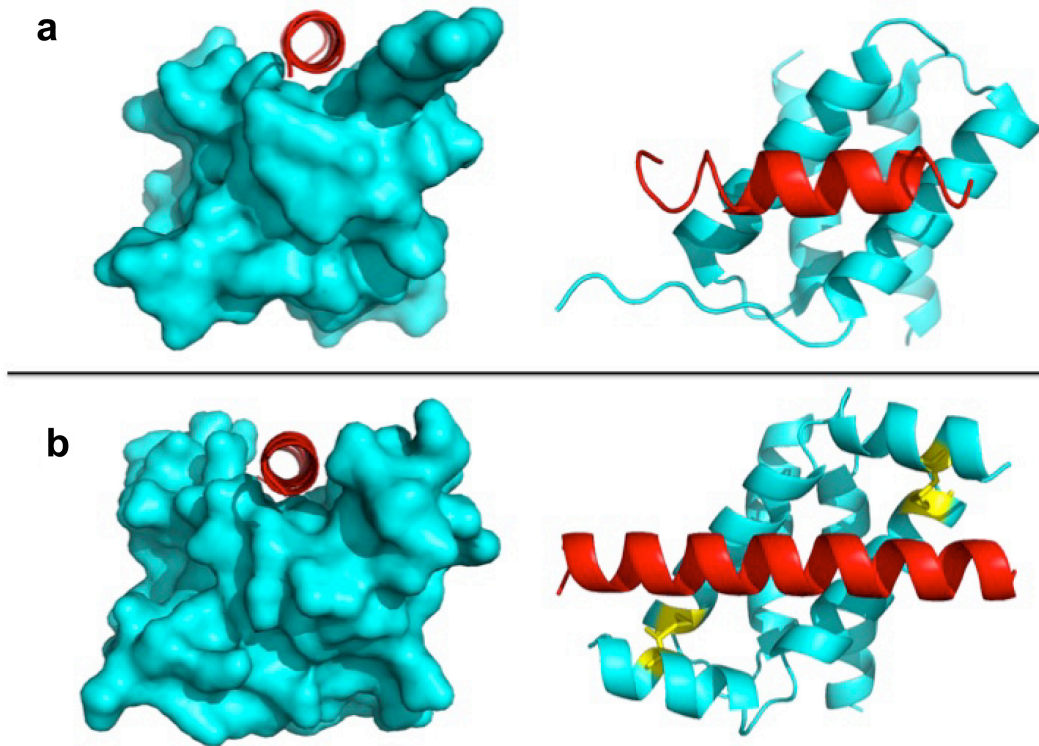


**Figure 1.4 Comparison of RII $\alpha$  D/D and RI $\alpha$  D/D.** Crystal structures of complex formed by AKB peptide with (a) RII $\alpha$  D/D or (b) RI $\alpha$  D/D are shown from two different angles. On the left, the RI $\alpha$  or RII $\alpha$  D/D is shown in spheres and colored in cyan. The different depths of the AKB docking groove formed by the two R D/D domains are highlighted. On the right, the RI $\alpha$  or RII $\alpha$  D/D is shown in cyan. The AKB peptide is shown in red for all four images. The two inter-chain disulfide bonds in RI $\alpha$  D/D are colored yellow. The images are modified based on structures from Kinderman. et al., 2006 (PDB: 2HWN) and Sarma. et al., 2010 (PDB: 3IM4) using Pymol.

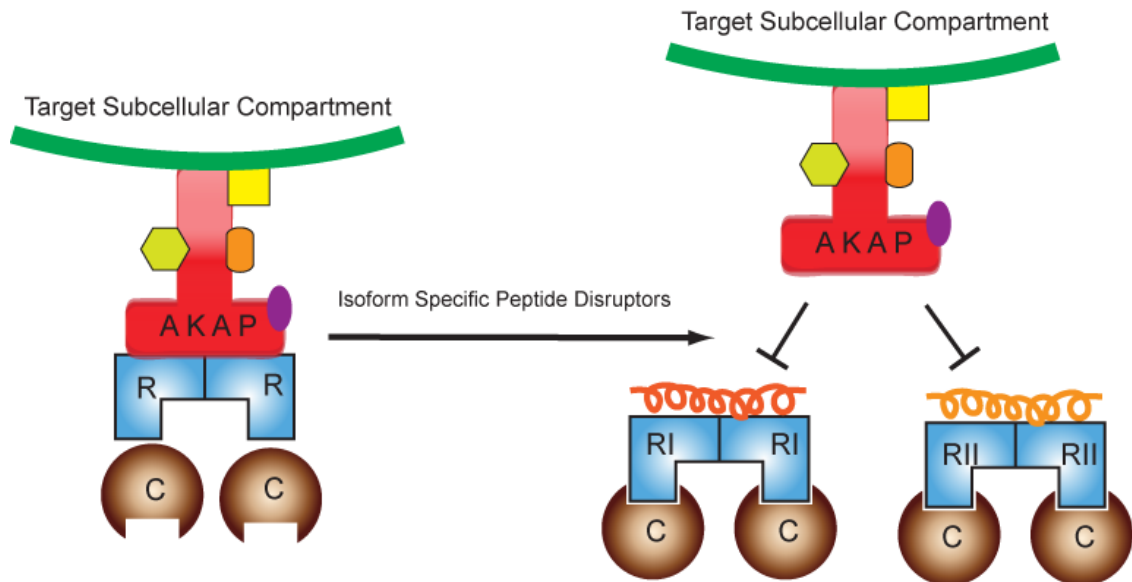


**Figure 1.5 Isoform-specific disruption of PKA signaling.** Isoform-selective peptides were designed to mimic the AKB helix, which is the region within AKAPs that interacts with PKA-R. Peptides were engineered to have specificity toward either isoform of PKA-R, thereby blocking downstream signaling through displacement of PKA-R from the AKAP signaling complexes.

**Table 1.1 Sequences of AKB sequences used as templates**

<b>Name</b>	<b>Sequence</b>
<b>AKB (RI)<sup>a</sup></b>	-FEE <b>LAWKIAKMIWSDVF</b> --
<b>AKB (RII)<sup>a</sup></b>	--EE <b>LLWKIAKMIVSDVM</b> --
<b>RIAD<sup>b</sup></b>	-LEQ <b>YANQLADQIIKEATE</b> -
<b>AKAP220<sup>c</sup></b>	-SIG <b>LANFLVSEALSNALK</b> -
<b>Human smAKAP<sup>d</sup></b>	VILEY <b>AHRLSQDILCDALQQ</b>
<b>Zebrafish smAKAP<sup>d</sup></b>	YAQ <b>RLSEEIVARAVQQWA</b> --
<b>SKIP<sup>e</sup></b>	FAEE <b>LADTVVSMATEIAAI</b> -

<sup>a</sup>AKB(RI) or (RII): A-Kinase Binding (RI) or (RII)[77];

<sup>b</sup>RIAD: RI-Anchoring Disruptor[78];

<sup>c</sup>AKAP220[79];

<sup>d</sup>smAKAP: small AKAP[47];

<sup>e</sup>SKIP: SPHK1-interacting protein[81].

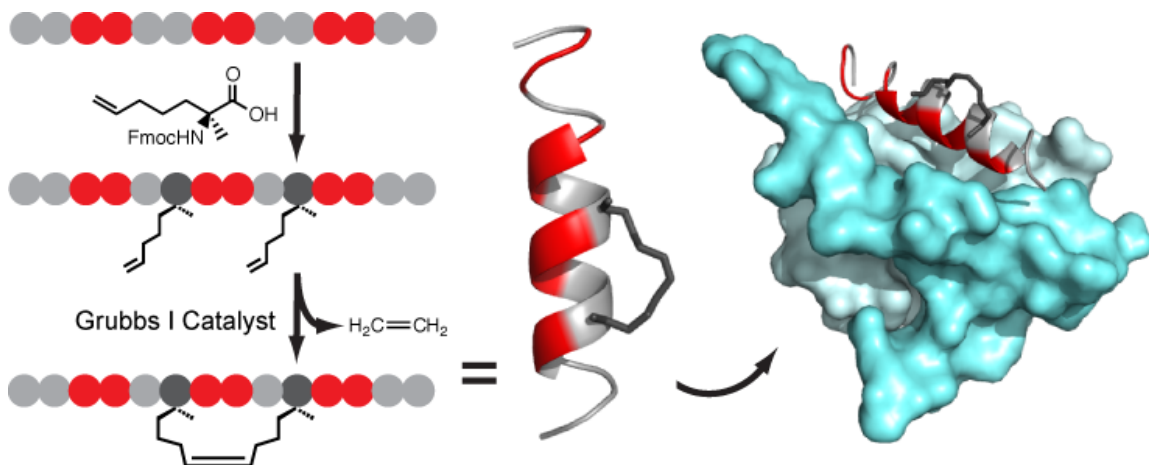


**Figure 1.6 Targeting R subunit using hydrocarbon stapled peptides.** Pairs of the non-natural amino acid S5 (shown in dark gray) are introduced into AKB or AKB-like sequences at  $i$  and  $i + 4$  positions. A hydrocarbon staple is formed by ring-closing olefin metathesis to form the conformationally constrained product. The hydrophobic residues that are essential for PKA-AKAP interactions (shown in red) were left unchanged. The engineered stapled peptide will target the AKB-binding site on the surface of the docking/dimerization (D/D) domain of PKA-R11 (shown in blue). The structure was rendered in PyMol using PDB ID 2HWN from Kinderman. et al., 2006.

CHAPTER 2

**RII-SELECTIVE DISRUPTION OF AKAP-LOCALIZED PKA  
USING HYDROCARBON STAPLED PEPTIDES**

---

Yuxiao Wang, Tienhuei G. Ho, Daniela Bertinetti, Matthias Neddermann, Eugen Franz, Gary C.H. Mo, Lewis P. Schendowich, Avinash Sukhu, Raybun C. Spelts, Jin Zhang, Friedrich W. Herberg and Eileen J. Kennedy. 2014, *ACS Chemical Biology*, 9, 635-642. Reprinted here with permission of publisher.

## **ABSTRACT**

A-kinase anchoring proteins (AKAPs) play an important role in the spatial and temporal regulation of protein kinase A (PKA) by scaffolding critical intracellular signaling complexes. Here we report the design of conformationally constrained peptides that disrupt interactions between PKA and AKAPs in an isoform-selective manner. Peptides derived from the A Kinase Binding (AKB) domain of several AKAPs were chemically modified to contain an all-hydrocarbon staple and target the docking/dimerization domain of PKA-R, thereby occluding AKAP interactions. The peptides are cell permeable against diverse human cell lines, are highly isoform-selective for PKA-RII and can effectively inhibit interactions between AKAPs and PKA-RII in intact cells. These peptides can be applied as useful reagents in cell-based studies to selectively disrupt AKAP-localized PKA-RII activity and block AKAP signaling complexes. In summary, the novel hydrocarbon-stapled peptides developed in this study represent a new class of AKAP disruptors to study compartmentalized RII-regulated PKA signaling in cells.

## INTRODUCTION

Protein Kinase A (PKA) or cAMP-Dependent Protein Kinase has broad substrate specificity and regulates a myriad of highly diverse cellular processes. Multiple mechanisms exist to fine-tune the spatial and temporal regulation of PKA on subcellular signaling [82-84]. The PKA holoenzyme complex is a tetramer composed of two catalytic subunits (PKA-C) and a regulatory subunit dimer (PKA-R). When intracellular cAMP levels increase, the PKA-R subunits bind cAMP and undergo a conformational change to release the catalytic subunits which then perform substrate phosphorylation [2, 85]. Regulation of PKA activity is partly controlled through the utilization of four distinct PKA-R subunit isoforms: PKA-RI (RI $\alpha$  and RI $\beta$ ) and PKA-RII (RII $\alpha$  and RII $\beta$ ). The PKA-R isoforms differ in many aspects including tissue expression, cAMP sensitivity and intracellular localization [82].

PKA activity is further regulated by a class of proteins called A Kinase-Ancoring Proteins (AKAPs) [84, 86]. The AKAP family is structurally diverse but shares the commonality of binding to PKA-R and compartmentalizing the PKA holoenzyme to multiple subcellular locations including the plasma membrane, endoplasmic reticulum and mitochondria [84]. AKAPs act as scaffolding proteins that tether PKA along with other proteins so as to integrate PKA activity into distinct multivalent signaling complexes. Other proteins tethered to these subcellular complexes include kinases, phosphatases, adenylyl cyclases, phosphodiesterases and various substrates [87-89]. By confining PKA to subsets of cellular substrates within a local cAMP environment, AKAPs provide

intrinsic specificity to cAMP-PKA signaling pathways and therefore act as key regulators for various cellular processes (Figure 1.2) [84, 86]. While most AKAPs preferentially bind to PKA-RII, several AKAPs have been identified that have PKA-RI specificity or can bind both PKA-RI and PKA-RII (dual specific) [51, 90]. Isoform-selective interactions appear to be critical for AKAP-mediated signaling since altered interactions between AKAPs and the PKA-R isoforms correlate with misregulated PKA activity and various disease states [47].

The significance of AKAP regulation on PKA activity is further underscored by its correlation with various disease phenotypes. Altered AKAP activity is implicated in many pathological processes including cardiovascular disorders, immune diseases and multiple cancer phenotypes [30, 91, 92]. While AKAPs are clearly important regulators of PKA, their full biological roles are largely elusive due to the complex nature of spatial and temporal regulation. In order to elucidate the role of AKAPs on localized PKA signaling, significant efforts have been put forth to block interactions between PKA and AKAP in a highly isoform-selective manner (Figure 1.5). One of the first peptide disruptors, Ht31, was derived from AKAP-Lbc and was subsequently modified to contain a stearylated moiety to allow for cell permeability [93]. Other peptides were also developed with improved properties including greater isoform specificity or higher binding affinities such as RIAD (RI-anchoring disruptor) [78] and SuperAKAP-IS [51]. Collectively, these peptides have become valuable tools to block PKA signaling mediated by either PKA-RI or PKA-RII PKA. However, there are still limitations with the physical properties of these compounds including poor cellular uptake by

intact cells, loss of the secondary structural fold in solution, and susceptibility to proteolytic degradation that is intrinsic to non-modified peptidyl bonds. Various modifications including addition of stearic acid [94], and additions of either a poly-arginine tag or HIV-1 TAT sequences [95, 96] have been utilized to improve cellular permeability. Nevertheless, many limitations still exist using these synthetic strategies including lack of reinforced secondary structure in solution, relatively short half-life values and potential mislocalization caused by the addition of conjugated sequences or moieties.

## **RESULTS AND DISCUSSION**

As an alternative strategy for the development of isoform-selective AKAP disruptors, we applied hydrocarbon peptide stapling. This chemical modification constrains the secondary structure of  $\alpha$ -helices through  $\alpha$ -methylation and macrocyclic ring formation (Figure 1.6) [74]. Further, this modification was found to increase the proteolytic stability of the peptide while also making it more entropically favorable for binding by locking it in a pre-binding state [97]. As a strategy to disrupt AKAP interactions, we focused on the conserved AKB helix that is shared among AKAPs. The AKB binds to the docking/dimerization (D/D) domain of PKA-R which is formed at the PKA-R dimer interface [45]. Crystallographic studies show that interactions between the amphipathic AKB peptides and the D/D domain of either PKA-RI or PKA-RII are predominantly driven by hydrophobic interactions [14, 15]. Many AKB or AKB-like sequences have been previously identified, however the majority of these sequences are

highly hydrophobic and therefore are limited in their potential as biochemical tools. We chose three intrinsically more hydrophilic sequences that target the AKB binding and used these as templates for generating hydrocarbon stapled peptide inhibitors: RIAD, AKAP220 and small membrane AKAP (smAKAP). In addition, the non-modified AKB sequences inherently have specificity for either PKA-RI or PKA-RII, thereby providing a basis for PKA-R isoform selectivity (Figure 1.5). Non-natural olefinic amino acids ((S)-2-(4'-pentenyl)alanine), abbreviated as S<sub>5</sub>, were introduced into the peptide sequences in *i*, *i*+4 positions (Figure 1.6). The olefinic amino acids were covalently crosslinked using ring closing metathesis chemistry [98, 99]. Libraries were generated where N- and C-terminal truncations were made to shorten the AKB sequence while preserving the hydrophobic residues of the binding interface (Figure 2.1, parent sequences). The hydrocarbon staples were introduced into various positions of the sequence by introducing the non-natural amino acids into positions on the solvent-exposed face of the helix (black residues). However, after introduction of the hydrocarbon staple into the parent sequences, these peptides had poor water solubility and therefore demonstrated minimal cell permeability (Figure 2.2). To remedy the limited cell permeability and solubility of these peptides, the AKB peptide mimics were optimized to increase their amphipathic properties through the addition of hydrophilic Lys residues on the solvent-exposed face of the helix (Figure 2.1, Lys-modified sequences). In addition, a short (PEG)<sub>3</sub> group was added to the N-terminus of the Lys-modified sequences to further improve water solubility.

Next, the binding affinities of the Lys-modified stapled peptides were measured using fluorescence polarization (FP) assays. Peptides were screened against the D/D domains of either RI $\alpha$  or RII $\alpha$  (Figure 2.3, 2.4, 2.5 and 2.6). The Lys-modified sequence lacking the addition of a hydrocarbon staple for each sequence was used as a control. Of the stapled peptides tested, none had an appreciable binding affinity for the PKA-RI subunit. Although the unmodified, original sequence of RIAD and smAKAP both demonstrate preferential binding to PKA-RI [47, 78], the chemically modified peptides are not as inherently flexible and therefore may have altered binding properties including its entropic and enthalpic properties. Nevertheless, multiple candidates were found that were highly selective for PKA-RII binding. Indeed, almost all of the peptides bearing a hydrocarbon staple at various positions were found to increase the binding affinity for PKA-RII $\alpha$ . Among all of the Lys-modified peptides tested, three were found that demonstrated  $K_D$  values in the low nM range: 1K-3 (2 nM), 2K-3 (6.2 nM) and 3K-5 (2.1 nM). Further, 1K-3 showed weak binding of PKA-RI $\alpha$  in the sub-micromolar range while 2K-3 and 3K-5 showed no appreciable binding affinities to PKA-RI $\alpha$ . These three promising candidates for highly selective disruption of PKA-RII were subsequently renamed Stapled Anchoring Disruptors (STADs; 1K-3 is STAD-1, 2K-3 is STAD-2 and 3K-5 is STAD-3). Stapled scrambled controls were also examined for each STAD peptide.

Next, the  $K_D$  values were measured for the three STAD peptides using full-length constructs human PKA-R (RI $\alpha$ , RI $\beta$ , RII $\alpha$  and RII $\beta$ ) since this would provide a more relevant portrayal of binding affinities and selectivity in the

context of human cells (Figure 2.7). Each of the isoforms was purified as previously described [100] and tested over a concentration range from 0.1 nM to 15  $\mu$ M. While all three peptides were found to have  $K_D$  values of 50 nM or less for PKA-RII $\alpha$ , STAD-1 also had a comparable affinity for PKA-RI $\alpha$  (93 nM). However, STAD-2 and STAD-3 interacted more weakly with PKA-RI $\alpha$  with STAD-2 having a  $K_D$  value of greater than 1  $\mu$ M and STAD-3 having a value of 144 nM. STAD-3 had the lowest  $K_D$  values for PKA-RII (8 nM for RII $\alpha$  and 16 nM for RII $\beta$ ). However, STAD-2 has a slightly reduced affinity compared to STAD-3 for PKA-RII (31 nM for RII $\alpha$  versus 64 nM for RII $\beta$ ), yet it has higher PKA-RII selectivity since STAD-2 binding to PKA-RII $\alpha$  is approximately 40 times more favorable than for PKA-RI $\alpha$ . Thus, it appears that STAD-2 and STAD-3 have the most pronounced isoform selectivity against full-length human constructs of PKA-RII by approximately one to two orders of magnitude as compared to PKA-RI.

With isoform selectivity and low  $K_D$  values confirmed, we next wanted to test the cellular uptake of these compounds. Three highly diverse human cell lines (HeLa, MDA-MB-231 and PC-3 cells) were treated with 5 $\mu$ M 5(6)-carboxyfluorescein labeled peptides for 6 hours before washing and fixation (Figure 2.8). While the non-stapled wild type control peptides for each peptide class were virtually impermeable to each of the cell types, STAD-1, STAD-2 and STAD-3 showed considerable intracellular access in all three cell lines. Further, although some punctate staining is evident, likely indicating intracellular localization in vesicles, particularly for STAD-3, there is a considerable amount of peptide localized in the cytoplasm and would therefore be accessible to AKAP-

PKA complexes. Of note, the original and stapled parent sequences were not cell permeable even after addition of a hydrocarbon staple (Figure 2.2), however the stapled STADs and their scramble control peptides were all cell permeable (Figure 2.8 and Figure 2.9). These observations indicate that addition of Lys residues on the hydrophilic face of the peptide was needed in order to promote cellular uptake of the peptide sequences.

Since the peptides appeared to have appreciable cytoplasmic localization, we wanted to determine whether they were physically interacting with PKA-R within the intracellular environment. In order to test this, we performed immunoprecipitation assays using MDA-MB-231 cells (Figure 2.10). Biotinylated STAD peptides (1 $\mu$ M) were added to the cell media 1 hour before lysis. Cells that were not peptide-treated were used as a control. Pull-downs were performed, followed by immunoblotting for either PKA-RI or PKA-RII. It is clear that both STAD-2 and STAD-3 interact with PKA-RII, while STAD-1 was found to weakly associate with PKA-RII in cells. None of the peptides appear to have any affinity for PKA-RI within cells. This experiment confirms that the STAD peptides are highly RII-selective even within the context of a cellular environment.

To determine whether the STAD peptides can effectively block PKA signaling in cells, we monitored PKA substrate phosphorylation in cells. MDA-MB-231 cells were serum-starved overnight, followed by pretreatment with different concentrations of STAD peptides for 1 hour prior to stimulation with 50  $\mu$ M forskolin (Fsk) to increase cAMP levels. Serum-starvation was performed to downregulate PKA activity so that a robust activation of PKA could be detected

upon stimulation of intracellular cAMP levels in the presence or absence of the STAD peptides. PKA activity was measured as a function of substrate phosphorylation using the anti-phospho-(Ser/Thr) PKA substrate antibody to detect phosphorylated PKA substrates in MDA-231 cells (Figure 2.11a). As a control, the small molecule inhibitor H89 (50  $\mu$ M) was used to inhibit PKA-C activity. Phosphorylation of CREB was also independently monitored since this is a known AKAP-mediated substrate of PKA [101]. All three STAD peptides decreased phosphorylation of various PKA substrates in a dose-dependent manner as compared to the forskolin-stimulated positive control. However, STAD-2 and STAD-3 appear to be more effective at inhibiting substrate phosphorylation as well as reducing phospho-CREB levels in these cell-based assays. Furthermore, the effect on substrate phosphorylation is not universal but rather some substrates are more impacted than others most notably under the lower 4  $\mu$ M treatment conditions. This suggests that phosphorylation of substrates that are regulated by signaling complexes involving AKAPs and PKA-RII are disproportionately reduced. To confirm that the peptide sequences are critical for targeted disruption of AKAP signaling complexes, scrambled versions of each STAD peptide were tested using the same assay. All three scrambled peptides had no apparent inhibitory effect on PKA signaling as measured by PKA substrate phosphorylation as well as phospho-CREB levels (Figure 2.11b). Taken together, these results suggest that STAD-2 and STAD-3 can be effectively localized within cells and can selectively disrupt AKAP-regulated signaling involving PKA-RII.

As a means of measuring the effects of the STAD peptides on AKAP-anchored versus non-anchored PKA activity, cytosolic PKA activity was probed using the diffusible biosensor AKAR4 in HeLa cells (Figure 2.12a and b) [102]. Cells treated with STAD-2 responded to Fsk (50  $\mu$ M)/IBMX (100  $\mu$ M) stimulation with a  $15 \pm 6\%$  (n=3) increase in yellow to cyan emission ratio, compared to a  $39 \pm 3\%$  (n=9) response from cells treated with the scramble control peptide. Using biosensor pmAKAR4 (targeted by a CAAX sequence), however, we found that STAD-2 could completely inhibit the sub-pool of PKA located at plasma membrane as compared to a non-peptide treated control (Figure 2.12c and Figure 2.13). The scramble STAD-2 control peptide did not alter the plasma membrane (Figure 2.12d) PKA responses in HeLa cells.

## **CONCLUSION**

In summary, we developed conformationally constrained, cell-permeable peptides that are highly selective for disruption of the interactions between AKAPs and PKA-RII. By conformationally constraining these AKAP inhibitor peptides, the binding interface is spatially poised to interact with the D/D of PKA-RII while also decreasing susceptibility to proteolytic degradation [74]. While AKAPs are important regulators of cAMP-mediated signaling in cells, there are still many unknowns regarding their roles in normal and disease-state signaling. This novel class of isoform-selective peptides targeting the AKAP binding site on PKA-R can be utilized as effective tools to selectively disrupt localized signaling

complexes mediated by interactions between AKAPs and PKA-RII and block downstream signaling in normal and disease-state cells.

## **METHODS**

### ***Materials***

The N- $\alpha$ -Fmoc protected amino acids and Rink Amide MBHA Resin were purchased from Novabiochem. (S)-N-Fmoc-2-(4'-pentenyl)alanine was purchased from Okeanos Tech. All other reagents and organic solvents used in this study were purchased from Fisher Scientific except where noted. HPLC grade methanol, acetonitrile and trifluoroacetic acid were used for all solutions involving preparation or analysis of samples.

### ***Cell Culture***

MDA-MB-231 and PC-3 cells were cultured in Roswell Park Memorial Institute-1640 (RPMI) Medium with L-glutamine (Lonza), 10% fetal bovine serum (Thermo Scientific) and penicillin/streptomycin (Amresco). HeLa cells were cultured in Dulbecco's Modified Eagle Medium (DMEM) with glucose and L-glutamine (Lonza), 10% fetal bovine serum (Thermo Scientific) and penicillin/streptomycin (Amresco).

### ***Peptide Synthesis***

Peptides were synthesized on Rink Amide MBHA resin using standard 9-fluorenylmethoxycarbonyl (Fmoc) solid phase synthesis. Deprotection steps

were performed using a 25% (v/v) solution of piperidine in 1-methyl-2-pyrrolidinone (NMP) for 30 minutes. For each coupling step, 10 equivalents of N- $\alpha$ -Fmoc protected amino acids (0.25 M final concentration in NMP) were added, followed by addition of 2-(6-chloro-1H-benzotriazole-1-yl)-1,1,3,3-tetramethylaminium hexafluorophosphate (HCTU, 0.23 M final concentration) in NMP and 8% (v/v) *N,N*-diisopropyl ethylamine (DIEA).

Olefin metathesis was performed using 0.4 equivalents of Bis(tricyclohexylphosphine) benzylidene ruthenium(IV) dichloride (Grubbs' first generation catalyst, Sigma Aldrich) relative to resin substitution. The reaction was performed in 1,2-dichloroethane at room temperature for 1 hour with agitation. The reaction was repeated once more using the same conditions to ensure complete conversion to the cyclized product. 11-amino-3,6,9-trioxaundecanoic acid (NH-PEG<sub>3</sub>-CH<sub>2</sub>COOH, ChemPep Inc.) was added to the N-terminus of all of the Lys-modified sequences and their scramble controls. The PEG<sub>3</sub> group was introduced using standard coupling conditions with 4 equivalents before the addition of biotin or 5(6)-carboxyfluorescein. N-terminal fluorescein labeling was performed using 2 equivalents of 5(6)-carboxyfluorescein (Acros Organics) along with 0.046 M HCTU and 2% (v/v) DIEA in *N,N*-dimethylformamide (DMF) overnight. N-terminal biotin labeling was performed using 10 equivalents of d-biotin (Anaspec), 0.14 M HCTU and 4% (v/v) DIEA in a 1:1 mixture of DMF and dimethyl sulfoxide (DMSO) overnight. Completed peptides were cleaved from resin using 95% trifluoroacetic acid, 2.5% water and 2.5% of triisopropylsilane (Sigma Aldrich) for 4-5 hrs, precipitated in

methyl-tert-butyl ether at 4 °C, and lyophilized. All peptides were purified by high-performance liquid chromatography (HPLC) and verified by mass spectrometry (MS). Fluorescein-labeled peptides were quantified by measuring absorbance of 5(6)-carboxyfluorescein at 495 nm using a Synergy 2 microplate reader (Bio-Tek). Biotin-labeled peptides were quantified by measuring decreased absorbance of the 2-Hydroxyazobenzen-4'-Carboxylic Acid (HABA)-avidin complex (VWR) at 500 nm.

The molecular weight of the purified peptides is as follows: 1K-wt = 2537.4 (expected mass = 2537.8); 1K-1 = 2531.4 (expected mass = 2531.9); 1K-2 = 2531.4 (expected mass = 2531.9); 1K-3 (STAD-1) = 2530.5 (expected mass = 2531.0); 1K-4 = 2530.5 (expected mass = 2530.9); 1K-3-scr (STAD-1 scr) = 2516.1 (expected mass = 2516.9); 2K-wt = 2461.2 (expected mass = 2461.9); 2K-1 = 2436.3 (expected mass = 2436.9); 2K-2 = 2435.1 (expected mass = 2436.0); 2K-3 (STAD-2) = 2454.0 (expected mass = 2455.0); 2K-3-scr (STAD-2 scr) = 2454.0 (expected mass = 2455.0); 3K-wt = 2862.0 (expected mass = 2862.3); 3K-1 = 2827.5 (expected mass = 2828.3); 3K-2 = 2827.5 (expected mass = 2828.3); 3K-3 = 2827.2 (expected mass = 2828.3); 3K-4 = 2828.4 (expected mass = 2828.4); 3K-5 (STAD-3) = 2984.1 (expected mass = 2984.5); and 3K-5-scr (STAD-3 scr) = 2983.4 (expected mass = 2984.5).

### ***Protein Expression and Purification***

The RI $\alpha$  docking/dimerization (D/D) domain (residues 1–61) of *Bos Taurus* and the RII $\alpha$  D/D (1-44) of *Rattus norvegicus* were expressed as previously

described [14, 55]. RI $\alpha$  D/D or RII $\alpha$  D/D cells were suspended and lysed in buffer containing 20 mM Tris (pH 8.0), 100 mM NaCl and 0.1 mM phenylmethanesulfonylfluoride (PMSF) before purification. The protein constructs were purified using a Talon cobalt-affinity resin (Clontech). Cobalt-purified proteins underwent further purification using a Superdex 75 (10 x 300 mm) size exclusion column (AKTA) on an AKTA Purifier UPC 10 (AKTA). Proteins were concentrated using Vivaspin 6 columns with a 3kDa molecular weight cutoff (GE Healthcare). Proteins were concentrated and 20% glycerol was added before being snap frozen in liquid nitrogen and stored at -80° C.

### ***Expression and Purification of Recombinant PKA-R Subunits***

Recombinant human PKA regulatory subunits (hRI $\alpha$ , hRI $\beta$ , hRII $\alpha$ , hRII $\beta$ ) were expressed and purified as previously described using Sp-8-AEA-cAMPS agarose [100]. SDS-polyacrylamide gel electrophoresis was used to monitor protein expression and purity. Typically, the recombinant proteins were purified to  $\geq$  95% homogeneity.

### ***Fluorescence Polarization using D/D Domain Constructs***

Fluorescence polarization (FP) assays were used to measure the binding affinity of designed peptides to the D/D domain of the PKA regulatory subunit isoforms. Each fluorescein-labeled peptide (10 nM) was plated with either RI $\alpha$  D/D or RII $\alpha$  D/D. The protein constructs were 10-fold serially diluted from 100 $\mu$ M to 0.1nM in 10 mM HEPES (pH 7.4), 0.15 M NaCl, 3 mM EDTA, and 0.005%

Surfactant P20. The plates were incubated in the dark at room temperature for 30 min. Fluorescence polarization was measured in triplicate using a Synergy 2 microplate reader (Bio-tek). Binding curves were generated and dissociation constants ( $K_D$ ) were calculated from the nonlinear regression curve using GraphPad Prism.

### ***Fluorescence Polarization using Full Length PKA-R***

To investigate the binding affinity of AKAP peptides to the full-length regulatory subunits of PKA, FP was applied in a direct assay format. Increasing concentrations (from 0.1 nM to 15  $\mu$ M) of the four different PKA regulatory subunits were mixed with 5 -10 nM fluorescently labeled AKAP peptide in 20 mM MOPS pH 7, 150 mM NaCl, 0.005% (v/v) CHAPS. Data were obtained using a Fusion<sup>TM</sup> alpha-FP plate reader at RT and a data acquisition of 2 seconds at Ex 485 nm / Em 535 nm in a 384 well microtiterplate (Perkin Elmer Optiplate, black). Data represent the mean  $\pm$  standard error of the mean of triplicate measurements (n = 3 per data point) for a single experiment.  $K_D$  determination was performed as described above.

### ***Cell permeability assays***

HeLa, MDA-MB-231 or PC-3 cells per well were seeded at 100,000 cells/well on 8-well tissue culture slides (BD Biosciences). Cells were grown overnight in medium with 10% fetal bovine serum. Next, 5  $\mu$ M 5(6)-carboxyfluorescein-labeled peptides were added and incubated at 37 °C for 6

hours before fixation in 2% paraformaldehyde. Slides were imaged using an Olympus X71 fluorescent microscope.

### ***Immunoprecipitation Assays***

MDA-MB-231 cells were pretreated with 1 $\mu$ M biotin-labeled peptides before being lysed in NP-40 buffer (20mM Tris-HCl, pH 8, 137mM NaCl, 10% glycerol, 1% Nonidet P-40, 2mM EDTA). Lysates were incubated with 50  $\mu$ L immobilized avidin resin (G-Biosciences) overnight at 4°C. The resin was collected by centrifugation at 1000\*g for 2 min, washed three times with NP-40 buffer and boiled in Laemmli sample buffer (60 mM Tris-Cl pH 6.8, 2% SDS, 10% glycerol, 5%  $\beta$ -mercaptoethanol, 0.01% bromophenol blue) at 95°C for 5 min. PKA-RI (1:500, BD Biosciences) and RII (1:1500, Abcam) antibodies were used for western blot detection. Anti-rabbit IRDye 800CW (1:25,000) and anti-mouse IRDye 680LT(1:30,000) secondary antibodies were used (LI-COR Biosciences). Blots were imaged using an Odyssey Fc imaging system (LI-COR Biosciences).

### ***Detection of Phosphorylated PKA Substrates***

MDA-MB-231 cells were grown on 12-well culture plate. Cells were serum-starved for 24 h in serum-free RPMI media with glutamine (0.3 g/L). Peptides were added to cell at either 2  $\mu$ M, 4  $\mu$ M or 8  $\mu$ M concentrations for 1 h, followed by stimulation with 50  $\mu$ M forskolin for 10 min. As a control, cells were treated with H89 (50  $\mu$ M) for 30 min prior to forskolin stimulation. Cells were lysed in Laemmli sample buffer and analyzed by western blotting. Anti phospho-

serine/threonine PKA substrate (1:1000, Cell Signaling Technology) or tubulin (1:2000, DSHB) primary antibodies were used, followed by anti-rabbit IRDye 800CW (1:25,000) or anti-mouse IRDye 680LT secondary antibodies (1:30,000) (LI-COR Biosciences). Blots were imaged using an Odyssey Fc imaging system.

### ***AKAR Reporter Assays***

The HeLa cells utilized for these experiments were between passages 60-61. Cells were maintained in DMEM growth media supplemented with 10% FBS, 1% penicillin and streptomycin. They were transfected with the appropriate biosensor at an approximate confluency of 70% using Lipofectamine 2000 reagent and incubated for 24 hours. Prior to imaging, cells were pretreated with 5  $\mu$ M of active or control peptides at 37°C in DMEM for 6 hours. They were then imaged in HBSS buffer supplemented with the corresponding peptide at room temperature.

Epifluorescence imaging was performed on a Zeiss Axiovert 200M Microscope equipped with a xenon lamp and a cooled CCD, under a 40X oil immersion objective. FRET microscopy of CFP/YFP biosensors was performed using the following excitation/emission filter combinations (bandwidths in nm): CFP – EX420/20, EM475/40; YFP – EX495/10, EM535/25; FRET: EX420/20, EM535/25. All epifluorescence experiments were subsequently analyzed using the MetaFluor software. All cells were analyzed, including those with visible blebbing or other morphological defects. Such cells typically present problems such as biosensor leakage and did not accurately reflect activity. They were

therefore rejected from reporting. The reported FRET ratio is calculated as follows and normalized with respect to the first frame in the time series ( $I$  = intensity):

$$\frac{I_{FRET} - I_{FRET,background}}{I_{CFP} - I_{CFP,background}}$$



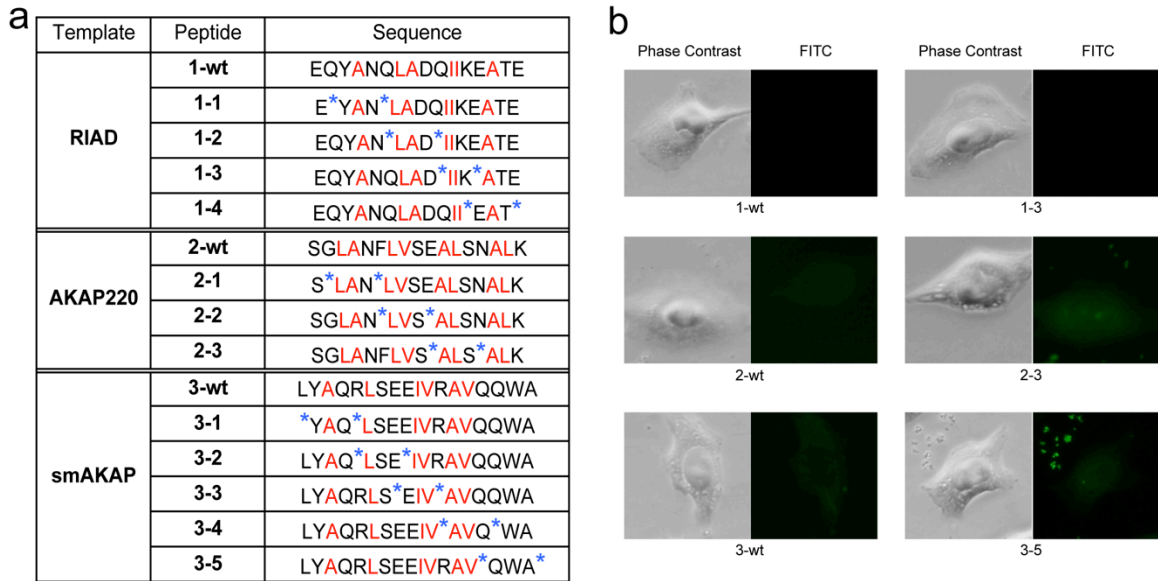


**Figure 2.2 Parent sequence peptides did not gain intracellular access. a)**

Library of parent sequence stapled peptides lacking the addition of Lys residues or an N-terminal PEG3 group. All peptides designed in the parent sequence libraries demonstrated limited water solubility. b) HeLa cells were treated with 5  $\mu$ M 5(6)-carboxyfluorescein labeled peptides of the original parent sequences in either a non-stapled or stapled format. Cells were pretreated with peptides for 6 hrs before washing, fixation and imaging by fluorescence microscopy. As expected, none of the compounds tested demonstrated notable cell permeability.

Peptide	Sequence	Rl $\alpha$ (nM)	Rll $\alpha$ (nM)		
<b>1K-wt</b>	KKYAKQLADQIIKEATE	> 1000	605 $\pm$ 190	STAD-1 wt	
<b>1K-1</b>	K*YAK*LADQIIKEATE	791 $\pm$ 237	105 $\pm$ 34		
<b>1K-2</b>	KKYAK*LAD*IIKEATE	353 $\pm$ 193	123 $\pm$ 62		
<b>1K-3</b>	KKYAKQLAD*IIK*ATE	<b>240 <math>\pm</math> 56</b>	<b>2.0 <math>\pm</math> 0.8</b>		STAD-1
<b>1K-4</b>	KKYAKQLADQII*EAT*	> 1000	232 $\pm$ 53		
<b>1K-3-scr</b>	AAEDYKIKI*LKT*QAK	> 1000	> 1000		
<b>2K-wt</b>	KKLAKFLVSEALKNALK	> 1000	22.4 $\pm$ 6.1	STAD-2 wt	
<b>2K-1</b>	K*LAK*LVSEALKNALK	> 1000	17.6 $\pm$ 7.0		
<b>2K-2</b>	KKLAK*LVS*ALKNALK	> 1000	28.7 $\pm$ 9.8		
<b>2K-3</b>	KKLAKFLVS*ALK*ALK	<b>&gt; 1000</b>	<b>6.2 <math>\pm</math> 2.0</b>	STAD-2	
<b>2K-3-scr</b>	KALVKLAAL*KFK*LKS	> 1000	> 1000		
<b>3K-wt</b>	KKYAQRLSKKIVRAVQQWA	> 1000	> 1000	STAD-3 wt	
<b>3K-1</b>	K*YAQ*LSKKIVRAVQQWA	> 1000	197 $\pm$ 110		
<b>3K-2</b>	KKYAQ*LSK*IVRAVQQWA	> 1000	> 1000		
<b>3K-3</b>	KKYAQRLS*KIV*AVQQWA	> 1000	356 $\pm$ 189		
<b>3K-4</b>	KKYAQRLSKKIV*AVQ*WA	> 1000	819 $\pm$ 383		
<b>3K-5</b>	KKYAQRLSKKIVRAV*QWA*	<b>&gt; 1000</b>	<b>2.1 <math>\pm</math> 0.6</b>		STAD-3
<b>3K-5-scr</b>	RVQKIVLRWKY AASQ*KAK*	> 1000	> 1000		

**Figure 2.3 Screening of Lys modified library using R D/D.** Fluorescence polarization assays of the Lys-modified peptide libraries were determined using purified protein constructs of the D/D domains from either PKA-RI or PKA-RII. S5 is represented using blue asterisk symbols. Peptides were plated at a final concentration of 10 nM, and the D/D dimerization domains were tested over a concentration range of 0.1 nM to 100  $\mu$ M. Dissociation constants were calculated using nonlinear regression and are presented as mean  $\pm$  standard error of triplicates. 1K-3 (STAD-1), 2K-3 (STAD-2), and 3K-5 (STAD-3) were identified as peptides with low  $K_D$  values for PKA-RII and were highly selective for PKA-RII over PKA-RI.

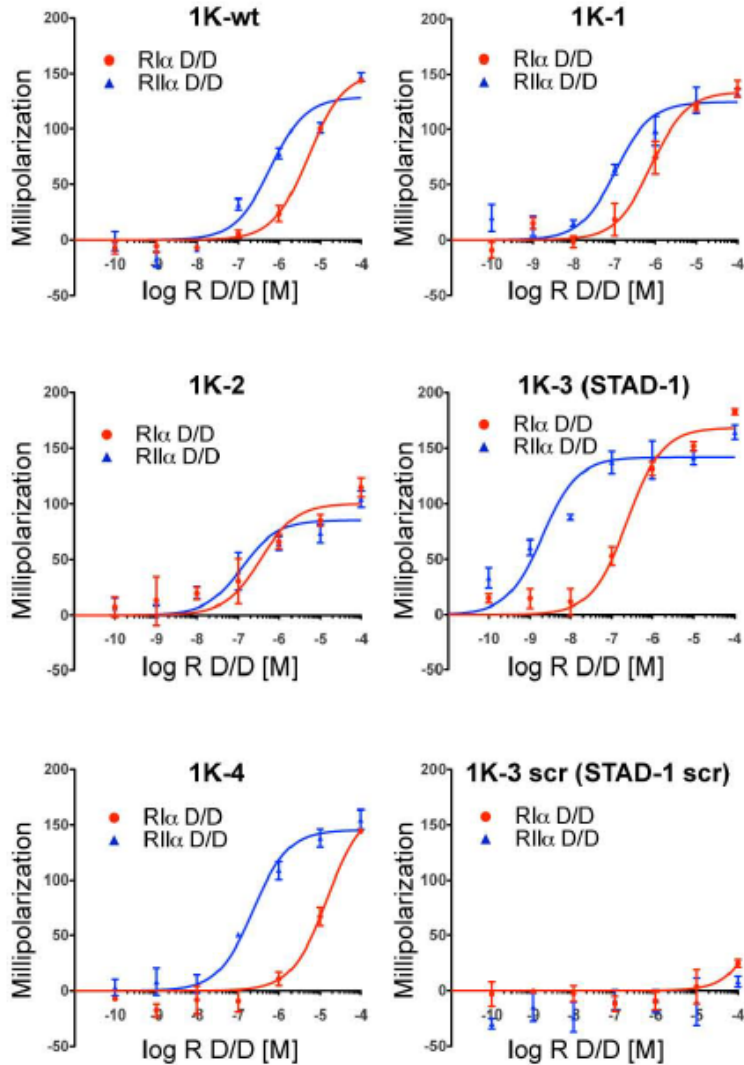


**Figure 2.4** Fluorescence polarization of 1K library of peptides. Binding curves of 1K peptides in **Figure 2.3**. Fluorescence polarization of the 1K Lys-modified peptide library was measured using purified protein constructs of the D/D domains from either PKA-R1 or PKA-RII. Peptides were plated at a final concentration of 10 nM and the D/D dimerization domains were tested over a concentration range of 0.1 nM to 100  $\mu$ M. Data was collected in triplicates for each concentration measurement.

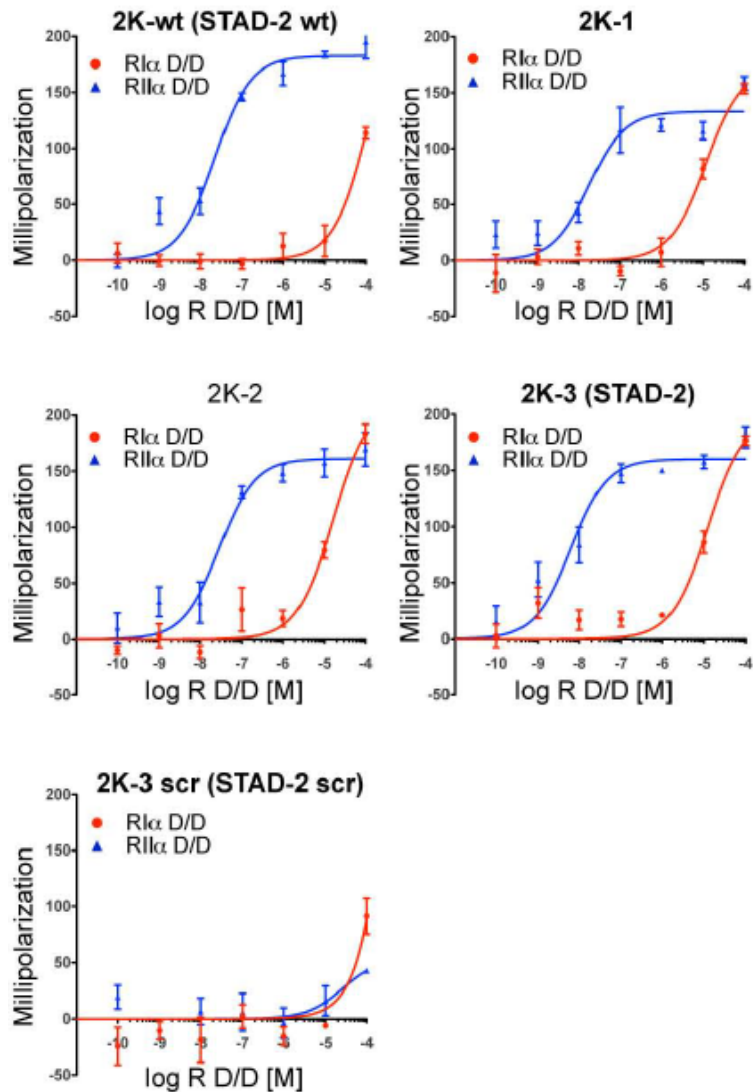


**Figure 2.5** Fluorescence polarization of 2K library of peptides. Binding curves of 2K peptides in **Figure 2.3**. Fluorescence polarization data of these peptides were measured using the same method described in **Figure 2.4**.

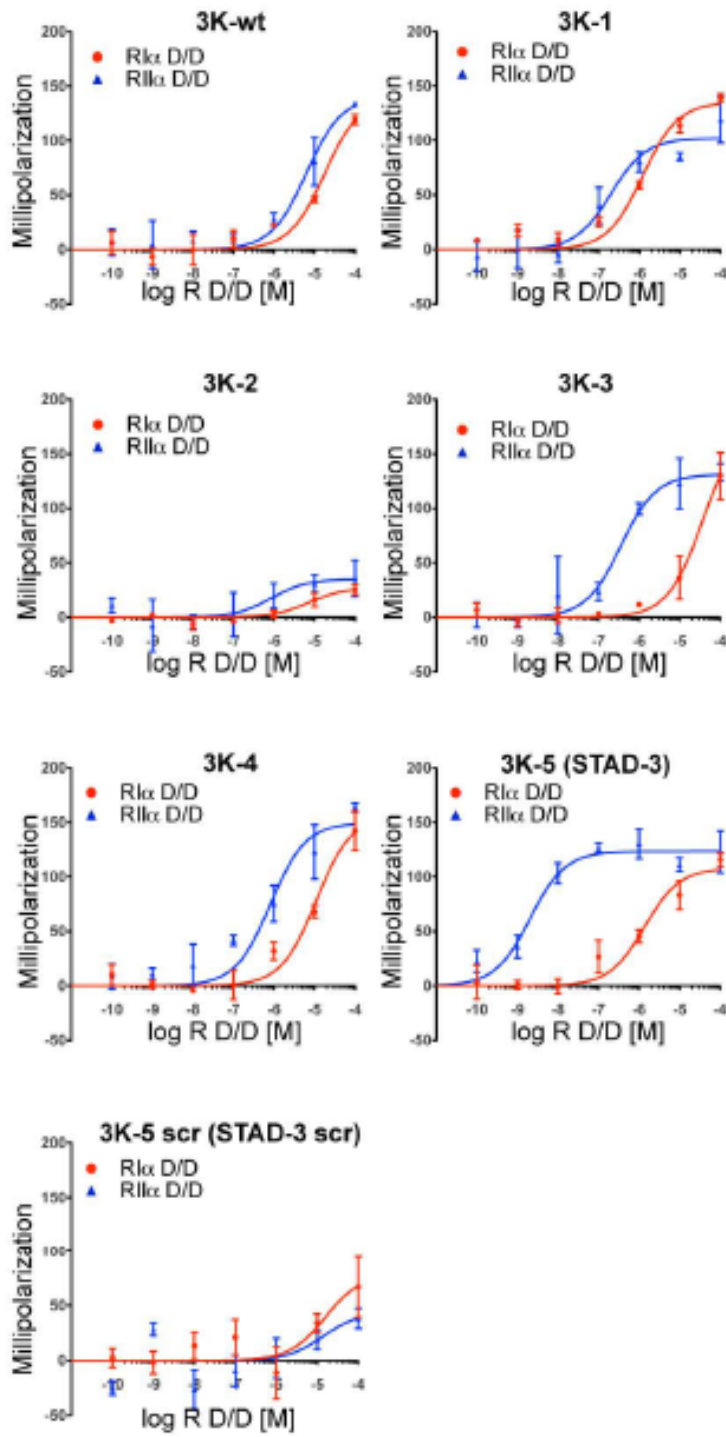


**Figure 2.6** Fluorescence polarization of 3K library of peptides. Binding curves of 3K peptides in **Figure 2.3**. Fluorescence polarization data of these peptides were measured using the same method described in **Figure 2.4**.

a

Peptide	$K_D$ (nM)		
	1K-3 (STAD -1)	2K-3 (STAD -2)	3K-5 (STAD -3)
hRI $\alpha$	93 $\pm$ 19 (n=5)	1,300 $\pm$ 122 (n=4)	144 $\pm$ 16 (n=4)
hRI $\beta$	131 $\pm$ 8 (n=4)	522 $\pm$ 52 (n=5)	97 $\pm$ 17 (n=6)
hRII $\alpha$	49 $\pm$ 12 (n=4)	31 $\pm$ 5 (n=4)	8 $\pm$ 1 (n=5)
hRII $\beta$	153 $\pm$ 11 (n=3)	64 $\pm$ 4 (n=3)	16 $\pm$ 2 (n=5)

b

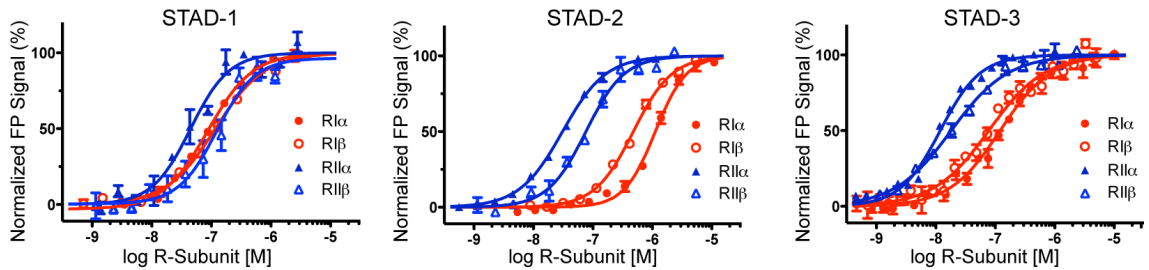


**Figure 2.7 Stapled peptides are highly selective for PKA-RII. (a)**

Fluorescence polarization was measured using full-length human proteins for each PKA-R isoform. Each single FP experiment was performed in triplicate. While all three peptides tested bound to PKA-RII $\alpha$  with a  $K_D$  value of 50 nM or less, STAD-2 and STAD-3 appear to have the greatest selectivity for PKA-RII binding over PKA-RI. (b) Normalized FP curves are shown for each of the full-length PKA R subunit isoforms. PKA-RI is represented in red (closed circles =  $\alpha$ , open circles =  $\beta$ ), and PKA-RII is shown in blue (closed triangles =  $\alpha$ , open triangles =  $\beta$ ). STAD-2 and STAD-3 show preference for PKA-RII binding by 1–2 orders of magnitude.

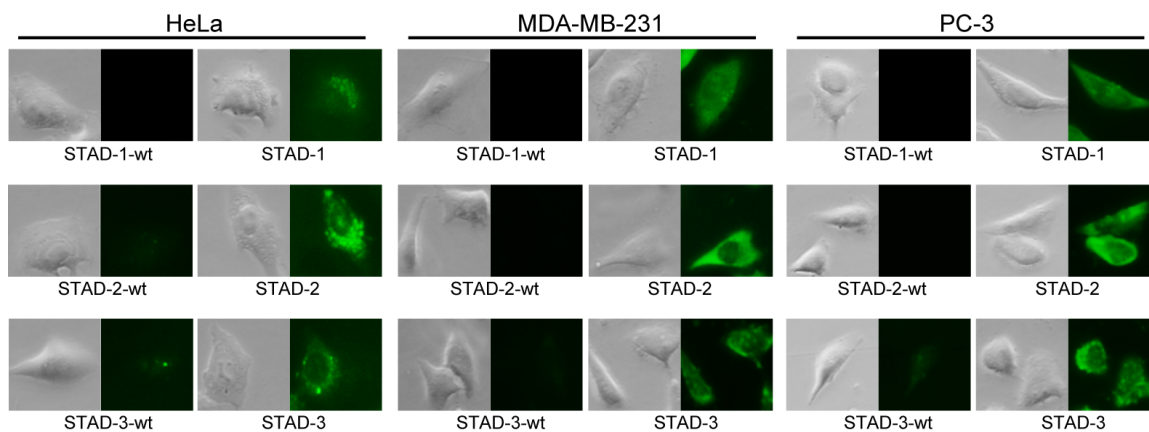


**Figure 2.8 Hydrocarbon staple significantly increases cell uptake.**

Fluorescent images of diverse cell lines (HeLa, MDA-MB-231, PC-3) after treatment with FITC-labeled peptides (5  $\mu$ M) for 8 h demonstrates that STAD-1, -2, and -3 are cell-permeable and have at least partial cytosolic localization. Each image is representative of three replicates.

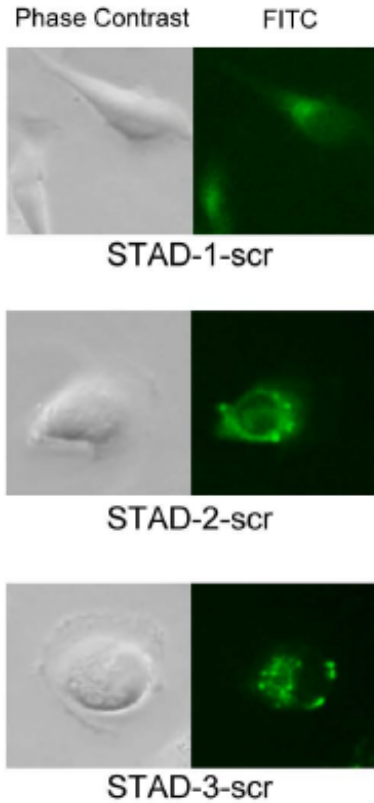


**Figure 2.9**      **Cell permeability of STAD scramble control peptides.** Cell permeability of the scramble controls for STAD-1, -2, and -3 were tested in MDAMB-231 cells. Cells were treated with 5  $\mu$ M of 5(6)-carboxyfluorescein-labeled peptides for 6 hrs before imaging. All three peptides were found to gain intracellular access to the cytoplasm.

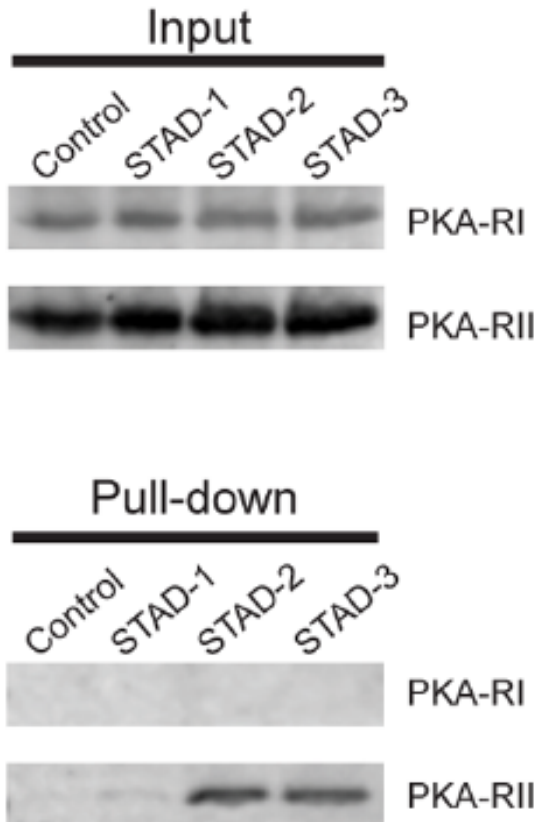


**Figure 2.10 STAD peptides can target RII in cells.** Immunoprecipitation experiments were performed in MDA-MB-231 cells. Cells were incubated with N-terminal biotin-labeled peptides (5  $\mu$ M) and pulled down by avidin-coated resin, and PKA-R1 and PKA-R2 were detected by immunoblotting. All three peptides demonstrated interactions with PKA-R2 to varying degree, while none showed any appreciable affinity for PKA-R1 in cells.

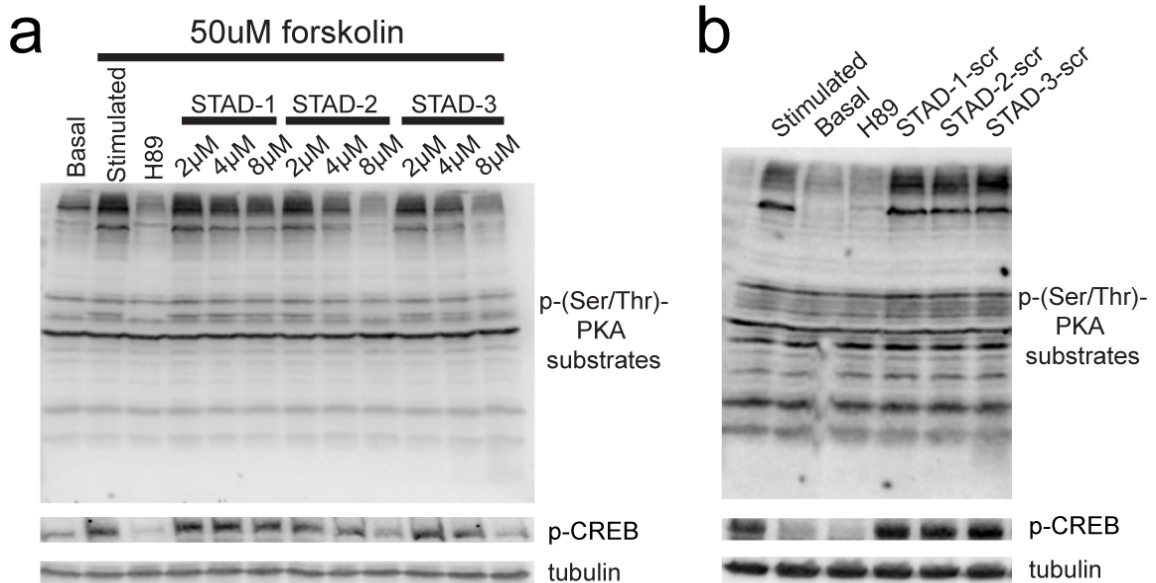


**Figure 2.11 STAD peptides can effectively block PKA signaling in cells.**

(a) The STAD peptides were found to cause dose-dependent disruption of PKA substrate phosphorylation. Cells were serum-starved, followed by stimulation with 50  $\mu$ M forskolin (except the basal lane). The PKA inhibitor H89 was used as a control (50  $\mu$ M). Phosphorylation of CREB was independently monitored to demonstrate that the peptides inhibit a known PKA substrate that is partly regulated by AKAP activity. The image is representative of three independent experiments. (b) STAD scramble peptides (8  $\mu$ M) were also monitored for their effects on PKA substrate phosphorylation. The scramble control peptides had no effect on PKA substrate phosphorylation or on CREB phosphorylation after forskolin stimulation.

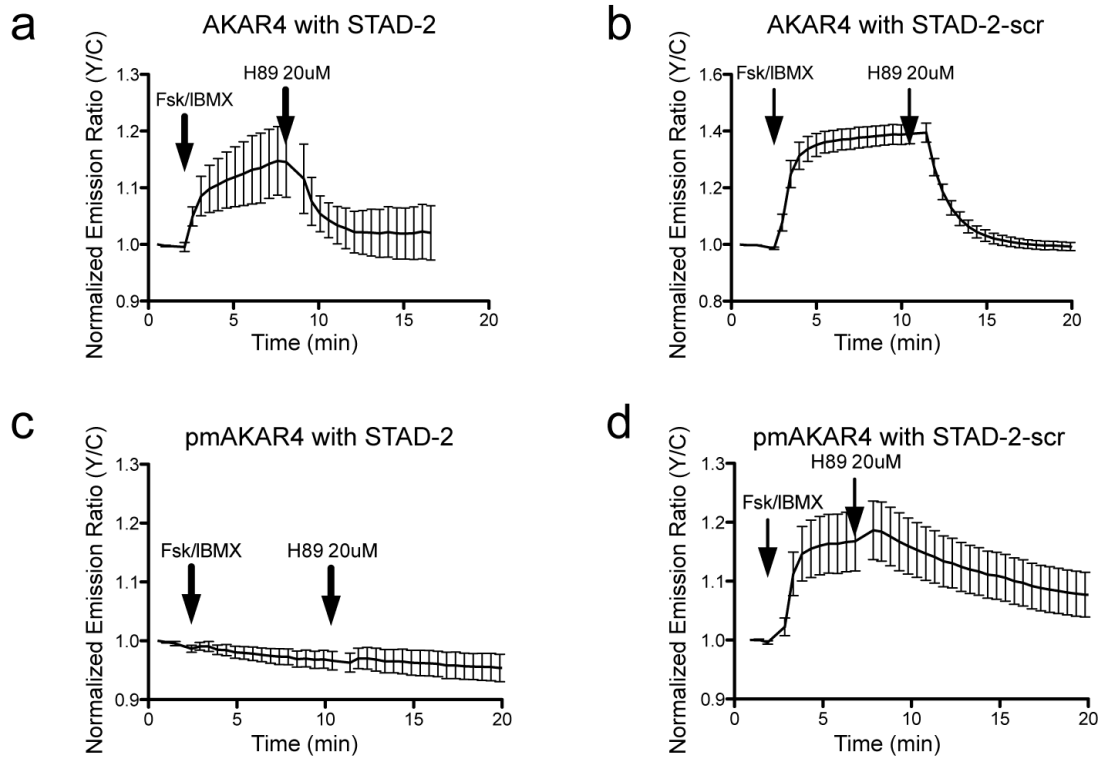


**Figure 2.12 STAD peptides affect only anchored PKA activity.** (a, b) Cytosolic PKA activity was monitored using the AKAR4 reporter. When treated with either STAD-2 or the STAD-2 scramble control, PKA activity was still stimulated by Fsk (50  $\mu$ M) and IBMX (100  $\mu$ M) and inhibited by H89 (20  $\mu$ M), indicating that STAD-2 does not affect nonlocalized PKA activity. (c, d) PKA activity localized near the plasma membrane was monitored using the pmAKAR4 reporter. In this instance, PKA activity was not stimulated by Fsk/IBMX or inhibited by H89 in the presence of STAD-2, indicating that STAD-2 selectively inhibits localized PKA activity. This effect was not evident when the pmAKAR4 reporter was tested with the STAD-2 scramble control.

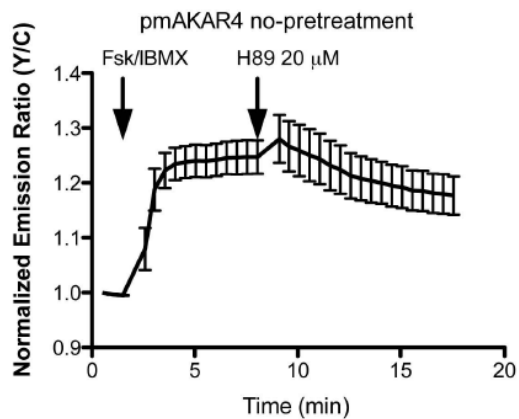


**Figure 2.13 PKA response in cells without peptide treatment.** The PKA response is shown in HeLa cells lacking peptide pretreatment using the pmAKAR4 probe. PKA activity is enhanced in response to Fsk/IBMX stimulation, and is inhibited by treatment with H89.

CHAPTER 3

**DISRUPTION OF AKAP-MEDIATED TYPE I PKA LOCALIZATION  
USING HYDROCARBON STAPLED PEPTIDES**

---

Yuxiao Wang, Tienhuei G. Ho, Daniela Bertinetti, Eugen Franz, Lewis P. Schendowich, Avinash Sukhu, Friedrich W. Herberg and Eileen J. Kennedy. To be submitted to *Journal of Biological Chemistry*

## ABSTRACT

Protein kinase A (PKA), a broad-spectrum kinase that is involved in a variety of cellular signaling, plays the role of a global regulator for many important cellular and physiological functions. Orchestration of such complex signaling is partially carried out by spatiotemporal regulation based on interaction of PKA regulatory subunits and A-kinase anchoring protein (AKAP). Delineation of PKA signaling requires utilization of disruptors to block RI or RII binding from AKAP, respectively. Here we report conformationally constrained peptides named Stapled RI Anchoring Disruptors (STRIADs) that target the RI docking/dimerization domain. These peptides have high binding affinity and specificity for the RI subunits *in vitro*. They are also cell-permeable and can effectively target RI but not RII in intact cells. Therefore, STRIADs are an invaluable tool to study localized type I PKA signaling events.

## INTRODUCTION

As the second messenger of intracellular propagation of hormone signaling, cAMP is involved in a plethora of downstream cellular and physiological events[103]. cAMP-dependent protein kinase (PKA) is the major intracellular target of cAMP and therefore works as a global regulator of many cellular processes such as cell proliferation, cell differentiation, cell death, metabolism and immune responses[104-106]. The inactive form of PKA is a heterotetramer composed of two regulatory subunits (R) and two catalytic subunits (C). Upon activation by cAMP, the two catalytic subunits are released from the two regulatory subunits and become available to phosphorylate substrates in close proximity. The signaling specificity of PKA is partially regulated through different isoforms of the regulatory subunit (RI $\alpha$ , RI $\beta$ , RII $\alpha$ , RII $\beta$ ), who vary in tissue distribution, cAMP responsiveness and especially subcellular localization[82]. RI isoform primarily diffuse in the cytoplasm although there are incidents that they can be recruited to specific subcellular compartments[17, 107, 108]. RII isoform, on the other hand, are mostly directed to various subcellular organelles through association with its membrane fraction[76]. Such diversification of subcellular compartmentalization is the basis of spatial regulation of PKA activity that is facilitated by A-Kinase Anchoring Proteins (AKAPs).

AKAPs are a family of structurally diverse scaffolding proteins that anchor PKA with its corresponding substrates to target subcellular sites, thereby promoting spatial fidelity and efficiency of signaling. At the same time, AKAPs

also exerts the temporal layer of regulation by tethering protein phosphatases, adenylyl cyclases and phosphodiesterases into one multi-protein complex with PKA[84, 86, 87, 109]. Therefore, AKAPs are the key spatiotemporal regulator that recruits different components to form a signaling complex which ensure PKA responds to local cAMP gradient and only phosphorylate the relevant substrates at only the right time[44, 45]. Initially, the majority of AKAPs identified only bind to RII tightly, while only some dual specific AKAPs, such as D-AKAP1[52], D-AKAP2[110] and AKAP220[79] have been shown to bind RI as well. It was not until recent years that RI-specific AKAPs like SKIP and smAKAP were identified[46, 47]. While much knowledge regarding the biochemical aspect of this family has been gained, the functional significance of these newly discovered AKAPs and their mechanism of signaling regulation remains elusive. To explore this area, development of isoform-specific disruptors that can selectively block RI- or RII- mediated anchoring is a promising approach.

Design of peptide disruptors was largely based on the A-Kinase Binding (AKB) domain, an amphipathic helix formed by 16-20 residues that bind to the PKA docking and dimerization domain of PKA-R[48]. Since the report of the prototypic disruptor Ht31 that is based on AKB of AKAP-Lbc, several peptides with high RII binding affinity and selectivity, such as AKAP-IS[75] and SuperAKAP-IS[51], were designed using *in silico* approaches. Unlike RII specific disruptors, progress in developing RI specific disruptors have been comparatively limited, probably due to the discriminating nature of RI D/D domain. The first peptide, PV-38, that preferentially interacts with RI was derived from the AKB

domain of D-AKAP2 using single amino acids substitution arrays[77]. In 2006, the design of a peptide called RI-anchoring disruptor (RIAD) was reported and has been widely used to study AKAP-RI interactions since then[78]. Although these sequences are valuable tools to block RI or RII mediated signaling, their *in cellulo* and *in vivo* applications are limited by the intrinsic disadvantages of non-modified peptides, including compromised secondary structure in solution, insufficient penetration through intact cell membrane and susceptibility to proteolytic degradation. Recently, our group developed a hydrocarbon-stapled peptide named stapled anchoring disruptor (STAD) that overcomes these issues and can selectively delocalize RII from AKAP in cell-based assays without manipulation of the cells[111]. Here we report a stapled RI anchoring disruptor (STRIAD) that can effectively inhibit interaction between AKAP and RI in intact cells.

## RESULTS

### ***RIAD as a template to develop hydrocarbon stapled RI anchoring disruptor***

Through the crystal structures of AKAP peptides in complex with RI $\alpha$  or RII $\alpha$  D/D domain, the similar binding mode shared by the two different isoforms may be appreciated. They both present an overall hydrophobic surface on the docking site that allows AKAP to bind diagonally across the two dimers[14, 15]. However, there are several differences that serve as the isoform-selective basis for different AKB sequences. First, compared to the shallow groove of RII $\alpha$  that easily accommodates most AKAPs, RI $\alpha$  D/D has a much deeper cleft and

therefore necessitates more specific criteria for AKAPs to bind[45, 112]. Another feature of RI $\alpha$  that limits the sequence recognition is the presence of two inter-chain disulfide bonds that covalently link the two monomers. These two crosslinks further restrict access of the docking cleft by decreasing the flexibility of the RI $\alpha$  D/D domain[12]. In addition to the shared hydrophobic interactions, hydrophilic residues also appear to play a role in the binding between RI $\alpha$  and AKAP. This is in contrast to the predominant hydrophobic nature of RII $\alpha$  docking surface[12]. As RI $\alpha$  is more discriminating in terms of AKB sequence, single point mutations of most residues easily abolishes RI $\alpha$  binding in a substitution array[77]. However, an aromatic residue at a specific site on the AKB sequence appears to favor the binding of RI $\alpha$  over RII $\alpha$  (Figure 3.1). This is reinforced by the presence of a cavity that can accommodate a bulky group in RI $\alpha$  but not in RII $\alpha$ [14]. Collectively, these differences of RI $\alpha$  and RII $\alpha$  D/D allow the isoform-specific disruption using peptides that mimic the AKB helix of AKAP.

RI-Anchoring Disruptor (RIAD), with the sequence LEQYANQLADQIIKEATE, is a peptide that exhibits an apparent 50-fold selectivity for RI $\alpha$  over RII $\alpha$ [78]. Based on the alignment of several RI binding AKAPs, Carson et al. designed the sequence using MEME algorithm analysis and guidance from single amino acids substitution array. RIAD is an amphipathic  $\alpha$ -helix with hydrophobic residues aligned on one side to form a hydrophobic patch, which is expected to interact with the hydrophobic groove of the RI D/D. The polar residues on the opposite side of the helix are exposed to water. Poly-arginine tagged RIAD was shown to successfully displace AKAPs from RI and

block downstream PKA signaling mediated by RI but not RII in cells. However, its application is still compromised by the lack of secondary structure in solution, relatively short half-life from proteolytic degradation and potential mislocalization due to conjugated moieties. To improve the biophysical and biochemical properties of RIAD, we adopted a helix-stapling strategy called hydrocarbon stapling to chemically constrain the peptide. A pair of non-natural olefinic amino acids ((S)-2-(4'-pentenyl)alanine), abbreviated as S5, were introduced into the sequences by replacing the residue at  $i$  and  $i + 4$  positions, but avoiding the key hydrophobic residues that are essential in preserving the interaction with RI. Ring-closing metathesis was then performed to crosslink the two olefinic side chains, forming the hydrophobic staple (Figure 3.2). Because of the positioning of the two S5 amino acids, the staple is at the water-exposed side of the helix and will not interfere with the protein-peptide interface. This method stabilizes an  $\alpha$ -helical structure through macrocyclization and  $\alpha$ -methylation, locking the peptide into a entropically favorable prebinding conformation[74, 98]. Peptides with this chemical modification were shown by several studies to possess enhanced  $\alpha$ -helicity, prolonged serum stability and a more drug-like properties *in vivo*[113, 114].

### ***Characterization of stapled RI-anchoring disruptor binding in vitro***

At first, four stapled peptides based on sequence of RIAD were designed. Non-modified RIAD is named as wild type (wt), while the stapled peptides are named as variant 1 through variant 4 (v1 to v4). Each stapled peptide has one

pair of S5 that flanks one of the four hydrophobic registers along the sequence of RIAD, forming the staple that spans one helical turn on the water-exposed side (Figure 3.2). However, these peptides did not have desirable aqueous solubility (data not shown), likely due to the additional hydrophobicity from the hydrocarbon staple. To address this issue, a mini-(PEG)<sub>3</sub> group was conjugated to the N-terminus of the sequence. Next, fluorescence polarization assays were used to determine the binding affinity on RI $\alpha$  and RII $\alpha$  D/D with 5(6)-carboxyfluorescein-labeled peptides (Figure 3.3 and 3.4). All four stapled peptides had increased binding affinities to both RI $\alpha$  and RII $\alpha$  D/D when compared to wt sequence, except for v4's binding to RI $\alpha$ . This is due to enhanced  $\alpha$ -helical prebinding conformation endowed by hydrocarbon stapling. However, the dissociation constants ( $K_D$ ) of the peptides binding to RII $\alpha$  generally had a larger decrease compared to RI $\alpha$ . This is not surprising given that RII $\alpha$  D/D is more tolerant to changes in AKAP sequences[77]. Nonetheless, v1 and v3 still showed tighter binding to RI $\alpha$  (12.05 nM and 1.49 nM, respectively) than RII $\alpha$  (34.65 nM and 2.57 nM, respectively). Ideal positioning of the hydrocarbon staple should not restrict the segment that needs some extent of flexibility for binding while locking the peptides into a pre-binding helical conformation. Since v1 has the highest selectivity (~3 folds), we further optimized the sequence by shifting the position of the staple to N or C-terminus by one residue (Figure 3.3). In the meantime, an additional lysine was added to the C-terminus of each v1-derived sequence in order to remedy the poor cellular uptake of v1 (Figure 3.5b). To our surprise, v1-2 showed a significant decrease of binding affinity to RII $\alpha$  compared

to v1 with the only difference between the two sequences being the additional lysine on the C-terminus of v1-2. This is probably due to incompatibility of the hydrophobic surface of RII $\alpha$  D/D and the polar side chain, as the added lysine (K19) is expected to be on the same side as the hydrophobic patch of the helix that faces R D/D (Figure 3.6). v1-1 showed very high affinity to both RI $\alpha$  (0.27 nM) and RII $\alpha$  (5.08 nM), indicating stapling at position 2, 5 is better than position 3, 7. At the same time, it also has a much higher selectivity (~19 fold) for RI $\alpha$  compared to v1, probably because of the effect of K19 at the C-terminus. v1-3, on the other hand, had no appreciable RI binding because the key bulky residue Tyr4 was replaced and the staple was partially interfering with the hydrophobic interface.

Peptides v3, v1-1 and v1-2 were subsequently designated as Stapled RI-Anchoring Disruptor (STRIAD; v3 is STRIAD-1, v1-1 is STRIAD-2, and v1-2 is STRIAD-3). To better depict the interaction between these peptides and PKA-R in a way more relevant to a human model, further binding assays using all four isoforms of full-length human PKA-R were carried out (Table 3.1 and Figure 3.7). All three peptides showed nanomolar affinity for RI $\alpha$  (5.8 nM, 6.2 nM and 7.3 nM) and decent affinity for RI $\beta$  (14.1 nM, 12.1 nm and 34.5 nM). Consistent with PKA-R D/D binding assay, STRIAD-1 also binds tightly to RII $\alpha$ , with K<sub>D</sub> of 19.4 nM. Its K<sub>D</sub> with RII $\beta$  is relatively high (166 nM), meaning STRIAD-1 is selective for RI $\alpha$ , RI $\beta$  and RII $\alpha$ . STRIAD-2 and STRIAD-3, on the other hand, both strongly prefer the binding of RI over RII. STRIAD-2 binds RI $\alpha$  26 times more favorable than RII $\alpha$  and 79 times more than RII $\beta$ . STRIAD-3 has the highest selectivity for RI

among the three peptides, with a preference for RI $\alpha$  by 58-fold as compared to RII $\alpha$  and 89-fold as compared to RII $\beta$ . Therefore, both STRIAD-2 and STRIAD-3 are high-affinity RI binders with significantly lower affinity for RII.

AKAPs are an extremely diverse family and not all AKAPs interact with PKA-R D/D through the amphipathic AKB domain. The few AKAPs that bind PKA-R via unconventional domains are called “noncanonical AKAPs”. For example, pericentrin interacts with RII through a non-helical, leucine-rich region that is 100 amino acids long[115].  $\alpha$ 4-integrin, another noncanonical AKAP, is RI-specific and insensitive to traditional amphipathic peptide disruptors[116]. Furthermore, several canonical AKAPs have an additional binding surface termed RI specifier region (RISR) outside the traditional amphipathic AKB domain. With multiple basic residues present, RISR is speculated to facilitate the stabilization of the AKAP-RI complex. Therefore, to ensure that STRIAD peptides genuinely target the RI subunits through the conventional mechanism of an amphipathic helix-helix interaction, a competition assay using the prototypic AKAP disrupter Ht31 was performed. Briefly, a range of unlabeled Ht31 was mixed with 4nM of fluorescently labeled STRIAD peptides and then incubated with RI $\alpha$  for 5 min prior to reading the FP signal. EC<sub>50</sub> values of Ht31 for STRIAD-1, -2 and -3 are 1.9  $\mu$ M, 2.1  $\mu$ M and 1.5  $\mu$ M, respectively (Figure 3.8). This is in line with the reported K<sub>D</sub> of 2.1  $\mu$ M for binding affinities between Ht31 and RI $\alpha$ [36]. Among the three peptides, STRIAD-2 is the tightest binder to RI $\alpha$  as it takes highest concentration of Ht31 to outcompete it. Another control competition assay showed that STRIAD-2 could not be replaced by Ht31PP from

R1 $\alpha$  up to 30  $\mu$ M (Figure 3.9). Ht31PP is the inactive analogue of Ht31 with two of its isoleucines substituted by prolines, which disrupts the essential helical conformation required by R D/D binding. This data suggests that STRIAD peptides indeed bind R1 $\alpha$  D/D by mimicking the amphipathic helical AKB of canonical AKAPs. It is also strengthened that these peptides have the potential as disruptors to replace type I PKA from endogenous AKAP under physiological conditions.

### ***STRIAD selectively disrupt PKA-R1 mediated signaling in cells***

As a prerequisite for an *in vitro* disruptor to become an *in cellulo* disruptor, they need to efficiently enter the cells. To test the cellular uptake of STRIAD peptides, MDA-MB-231 and PC-3 cells were treated with 5  $\mu$ M 5(6)-carboxyfluorescein-labeled peptides for 7 or 21 hours prior to washing and fixation. As a previous study has shown, hydrocarbon stapling drastically increased the ability of helical peptides to permeate through intact cell membrane[111]. Indeed, all three peptides showed considerable intracellular access after 7 hours of treatment as compared to wt (Figure 3.10, 3.11 and 3.5a). Although, there is an apparent punctate pattern in the cells, an increase of basal cytoplasmic level of fluorescein staining can be seen upon longer incubation.

With cell uptake established, biotin pull-downs were then performed to see if these peptides could successfully target PKA-R *in cellulo*. We treated MDA-

MB-231 cells with biotin-labeled STRIAD-1, -2 or -3 and then co-precipitated the lysates with avidin-coated resin, followed by immunoblotting for PKA-RI or RII. Whole cell lysates were also blotted as control. Compared to a non-treated control, STRIAD-1 and STRIAD-2 successfully pulled down PKA-RI, while no apparent interaction with RII was observed (Figure 3.12). A small amount of RI or RII was detected in precipitates from STRIAD-3 treated cells. Based on this set of data, we are able to confirm that STRIAD-1 and -2 are promising RI-selective disruptors in the context of a cellular environment.

## **DISCUSSION**

Despite the similar domain organization, R subunit isoforms are not functionally redundant. Besides the difference in subcellular localization in the cells, extended physiological significance of RI has been demonstrated by numerous studies in different models. RI $\alpha$  is unique among all four isoforms because it serves to compensate and inhibit unregulated catalytic activity when other isoforms are knocked-out[31]. RI $\alpha$  knockouts in mice leads to embryonic lethality, further showing that it is essential in early development[117]. Overexpression of RI $\alpha$  has been documented to play a role in malignant transformation[118]. In addition, patients of familial cardiac myxomas and Carney complex are mapped to the mutation of RI $\alpha$ [42, 119]. In line with these findings, a disease-susceptible single nucleotide polymorphism (SNP) in the AKB domain of D-AKAP2 has been associated with a higher risk of familial breast cancer, colorectal cancer and cardiac dysfunctions, highlighting the importance of PKA

localization in pathological conditions[63, 69, 72, 120]. Interestingly, even though D-AKAP2 binds both RI and RII with appreciable affinities, this SNP only affected RI but not RII interactions. However, the exact role of RI in the physiological and pathological conditions above is mostly unknown and the exact mechanism of its regulated by AKAP-mediated localization remains elusive. By blocking RI binding from AKAPs using STRIADs, the direct and downstream cellular effect of localized type I PKA signaling in a variety of disease systems can be studied.

Together with the RII-selective disruptor we reported earlier, STAD-2 and STRIAD-2 will serve as useful probes to dissect the respective role of AKAP-mediated type I and type II PKA signaling. Furthermore, we can also identify the primary targets of the two PKA isozymes and the involved signaling pathway with the help of other biochemical approaches and powerful tools like proteomics. More importantly, the application of stapled peptides is not only limited to cell-based assay. A hydrocarbon stapled peptide developed by Walensky et al. successfully bound to the multidomain BCL-2 member pockets and inhibited the growth of human leukemia xenografts *in vivo*[113]. As our stapled peptides have significantly increased stability in the presence of immobilized proteases (data not shown), we can take advantage of the enhanced pharmacological properties of the stapled peptides and study the functional differences of compartmentalized type I or type II PKA signaling *in vivo* without complicated genetic manipulations.

In this study, we report conformationally constrained helical peptides, STRIAD-1 and STRIAD-2, which can be used to selectively disrupt the interactions between AKAPs and PKA-RI. Cell-based experiments have shown

these peptides have favorable cellular permeability and can effectively target RI in intact cells. Therefore, STRIAD is a powerful and convenient tool that can be used to study AKAP-mediated type I PKA signaling in cells.

## **METHODS**

### ***Materials***

The N- $\alpha$ -Fmoc protected amino acids and Rink Amide MBHA resin used for peptide synthesis were purchased from Novabiochem. (S)-N-Fmoc-2-(4'-pentenyl)alanine was purchased from Okeanos Tech. All other reagents and organic solvents used in this study were purchased from Fisher Scientific except where noted. All reagents and solvents used in preparation or analysis of peptides such as methanol, acetonitrile, and trifluoroacetic acid, were HPLC grade pure.

### ***Peptide Synthesis***

9-fluorenylmethoxycarbonyl (Fmoc) solid phase synthesis was used to synthesize all of the peptides used in this study. First, Rink Amide MBHA resin was equilibrated in 1-methyl-2-pyrrolidinone (NMP) for 15 min. Deprotection was then performed using a 25% (v/v) solution of piperidine in NMP for 30 min, followed by three brief washes in NMP. For coupling of amino acid, 10 equiv of N- $\alpha$ -Fmoc-protected amino acids (0.25 M final concentration in NMP) were added, followed by addition of 2-(6-chloro-1H-benzotriazole-1-yl)-1,1,3,3-tetramethylammonium hexafluorophosphate (HCTU, 0.23 M final concentration) in

NMP and 8% (v/v) N,N-diisopropyl ethylamine (DIEA). Another three washes in NMP were performed after 45 min of coupling. Deprotection and coupling steps described above were performed for each amino acid until the full sequence was completed.

Olefin metathesis was then performed, if the sequence include S5, using 0.4 equiv. bis-(tricyclohexylphosphine) benzylidene ruthenium(IV) dichloride (Grubbs' first generation catalyst, Sigma Aldrich) relative to resin substitution. The reaction was performed in 1,2-dichloroethane at room temperature with agitation for 1 h. To ensure complete reaction, the metathesis was repeated once more using the same conditions. Next, 11-Amino-3,6,9-trioxaundecanoic acid (NH-PEG3-CH<sub>2</sub>COOH, ChemPep Inc.) was added to the N-terminus using standard coupling conditions with 4 equivs. Finally, the addition of an N-terminal biotin or 5(6)-carboxyfluorescein was performed. For fluorescein labeling, 2 equiv of 5(6)-carboxyfluorescein (Acros Organics) along with 0.046 M HCTU and 2% (v/v) DIEA in N,N-dimethylformamide (DMF) were added and allowed agitating overnight. For biotin labeling, 10 equiv of D-biotin (Anaspec), 0.14 M HCTU, and 4% (v/v) DIEA in a 1:1 mixture of DMF and dimethyl sulfoxide (DMSO) were added and allowed agitating overnight. Completed peptides were then cleaved from resin by agitating in 95% trifluoroacetic acid, 2.5% water, and 2.5% of triisopropylsilane (Sigma Aldrich) for 4–5 h. Upon completion, the reaction was precipitated in methyl-tert-butyl ether at 4 °C, and lyophilized. Peptides were suspended in methanol and purified by high-performance liquid chromatography (HPLC) and verified by mass spectrometry (MS). Fluorescein-labeled peptides

were quantified by measuring absorbance of 5(6)-carboxyfluorescein at 495 nm using a Synergy 2 microplate reader (Bio-Tek). Biotin-labeled peptides were quantified by measuring decreased absorbance of the 2-hydroxyazobenzen-4'-carboxylic acid (HABA)-avidin complex (VWR) at 500 nm.

The molecular weights of the purified peptides are as follows: wt = 2637.4 (expected mass = 2637.8); v1 = 2631.0 (expected mass = 2631.9); v2 = 2631.2 (expected mass = 2631.9); v3 (STRIAD-1) = 2616.4 (expected mass = 2616.9); STRIAD-1-scr = 2616.2 (expected mass = 2616.9); v4 = 2615.6 (expected mass = 2616.9); v1-1 (STRIAD-2) = 2758.2 (expected mass = 2759.1); STRIAD-2-scr = 2758.4 (expected mass = 2759.1); v1-2 (STRIAD-3) = 2745.4 (expected mass = 2745.4); STRIAD-3-scr = 2745.6 (expected mass = 2746.1); v1-3 = 2725.8 (expected mass = 2726.0).

### ***Protein Expression and Purification***

The RI $\alpha$  docking/dimerization (D/D) domain (residues 1–61) of *Bos taurus*, RII $\alpha$  D/D (1–44) of *Rattus norvegicus*, human PKA regulatory subunits (hRI $\alpha$ , hRI $\beta$ , hRII $\alpha$ , hRII $\beta$ ) were expressed as previously described[100, 111]. For RI $\alpha$  or RII $\alpha$  D/D, cells induced by 1 mM Isopropyl  $\beta$ -D-1-thiogalactopyranoside (IPTG) at 37 °C for 3 h were suspended and lysed in buffer containing 20 mM Tris (pH 8.0), 100 mM NaCl, and 0.1 mM phenylmethanesulfonyl fluoride (PMSF) before purification. The protein constructs were subsequently purified using a Talon cobalt-affinity resin (Clontech) and a Superdex 75 (10 mm  $\text{\AA}$ ~ 300 mm) size exclusion column (AKTA) on an AKTA Purifier UPC 10 (AKTA). Proteins were

concentrated using Vivaspin 6 columns with a 3 kDa molecular weight cutoff (GE Healthcare). 20% glycerol was added to concentrated proteins before being snap frozen in liquid nitrogen and stored at  $-80^{\circ}\text{C}$ . For full-length recombinant human PKA regulatory subunits (hRI $\alpha$ , hRI $\beta$ , hRII $\alpha$ , hRII $\beta$ ), Sp-8-AEA-cAMPS agarose packed column was used for purification. SDS-polyacrylamide gel electrophoresis (SDS-PAGE) was used to monitor protein expression and ensure purity to  $\geq 95\%$  homogeneity.

### ***Fluorescence Polarization Using PKA-R D/D Domain***

On a 96-well plate (Corning), 10 nM fluorescein-labeled peptides were plated with either RI $\alpha$  D/D or RII $\alpha$  D/D. The protein constructs were 10-fold serially diluted from 100  $\mu\text{M}$  to 0.1 nM in 10 mM HEPES (pH 7.4), 0.15 M NaCl, 3 mM EDTA, and 0.005% Surfactant P20. The plates were incubated in the dark at room temperature for 30 min before measured using a Synergy 2 microplate reader (Biotek). Experiments were performed in triplicates. Binding curves were generated, and dissociation constants ( $K_d$ ) were calculated from the nonlinear regression curve using GraphPad Prism.

### ***Fluorescence Polarization Using Full-length PKA-R***

A range of concentrations (from 60 pM to 10  $\mu\text{M}$ ) of the four full-length different PKA regulatory subunits were incubated with 4 nM fluorescently labeled STRIAD-1, -2 and -3 peptides in 20 mM MOPS pH 7, 150 mM NaCl, 0.005% (v/v) CHAPS. Data were obtained using a Fusion<sup>TM</sup> alpha-FP plate reader at

room temperature and a data acquisition of 2 s at Ex 485 nm/Em 535 nm in a 384 well microtiterplate (Perkin-Elmer Optiplate, black). Data represent the mean  $\pm$  standard error of the mean of triplicate measurements (n = 3 per data point) for a single experiment. Kd determination was performed as described above.

### ***Cell Culture***

MDA-MB-231 and PC-3 cells were cultured in Roswell Park Memorial Institute-1640 (RPMI) Medium with L-glutamine (Lonza), 10% fetal bovine serum (Thermo Scientific), and penicillin/streptomycin (Amresco). Cells grown to 80% confluency were either seeded to perform an assay or split 1:10 to a new dish.

### ***Cell Permeability Assays***

MDA-MB-231 or PC-3 cells were seeded at 8,000 cells/well on 8-well tissue culture slides (BD Biosciences). Cells were incubated overnight in growth medium before treatment of 5  $\mu$ M 5(6)-carboxyfluorescein-labeled peptides for 7 or 21 hours at 37 °C. When treatment is done, cells were fixed in 2% paraformaldehyde and imaged using an Olympus X71 fluorescent microscope. Each experiment was performed in duplicates.

### ***Biotin Pull-down Assays***

MDA-MB-231 cells grown to sub-confluency were treated with 5  $\mu$ M biotin-labeled peptide for 12 h and then lysed in lysis buffer (20 mM 4-(2-hydroxyethyl)-1-piperazineethanesulfonic acid (Hepes), 150 mM NaCl, 1 mM EDTA, 1% Triton

X-100, pH 7.5). Lysates were then incubated with 100uL immobilized avidin resin (G-biosciences) with rocking at 4 °C for 6 hours. Resins were collected by centrifugation at 1000\*g for 2min and washed three times with phosphate buffered saline (PBS) before boiling in laemmli sample buffer (60 mM Tris-Cl pH 6.8, 2% SDS, 10% glycerol, 5%  $\beta$ -mercaptoethanol, 0.01% bromophenol blue) at 95°C for 5min. PKA-RI (1:450)(BD Biosciences) and RII (1:2000)(Abcam) antibodies were used for the immunoblot analysis. Anti-rabbit (1:25,000) and anti-mouse were used correspondingly as secondary antibodies (1:30,000) (LI-COR Biosciences). The blot was then imaged using Odyssey Fc imaging system (LI-COR Biosciences).

### ***Ht31 Competition Assay***

Increasing concentrations of Ht31 or Ht-31PP (ranging from 15 nM to 30  $\mu$ M) were mixed with 4 nM of the indicated fluorescent labelled peptides. The mixture was incubated with R1 $\alpha$  whose concentration was adapted to 70 % of the maximum value derived from the direct full-length FP assay. Fluorescence polarization was measured after 5 minutes. Data were obtained using a Fusion<sup>TM</sup> alpha-FP plate reader at room temperature and a data acquisition of 2 s at Ex 485 nm/Em 535 nm in a 384 well microtiterplate (Perkin-Elmer Optiplate, black). Data were analyzed with GraphPad Prism 5.0 (GraphPad Software) by plotting the resulting polarization signal or the normalized polarisation signal against the logarithm of the Ht31 concentration.

RI-specific	AKAP-CE :	LYQ <b>F</b> AD <b>R</b> F <b>S</b> EL <b>V</b> ISE <b>A</b> LN <b>H</b>
	SKIP :	ITD <b>F</b> AE <b>E</b> L <b>A</b> DT <b>V</b> V <b>S</b> M <b>A</b> TE <b>I</b>
	smAKAP :	ILE <b>Y</b> A <b>H</b> R <b>L</b> S <b>Q</b> D <b>I</b> L <b>C</b> D <b>A</b> L <b>Q</b> Q
	RIAD :	LEQ <b>Y</b> A <b>N</b> Q <b>L</b> A <b>D</b> Q <b>I</b> I <b>K</b> E <b>A</b> T <b>E</b> -
RII-specific	AKAP-Lbc :	GAD <b>L</b> IE <b>E</b> A <b>A</b> S <b>R</b> I <b>V</b> DA <b>V</b> IE <b>Q</b>
	AKAP95 :	PEE <b>V</b> A <b>A</b> D <b>V</b> L <b>A</b> E <b>V</b> IT <b>A</b> A <b>V</b> R <b>A</b>
	AKAP79 :	YET <b>L</b> L <b>I</b> ET <b>A</b> S <b>S</b> L <b>V</b> K <b>N</b> A <b>I</b> Q <b>L</b>

**Figure 3.1 Alignment of several RI- and RII-specific AKAP sequences.** The four hydrophobic registers shared by all sequences are highlighted in green. The aromatic residues shared by RI-specific sequences are highlighted in blue. Reference: AKAP-CE [53], SKIP [46], smAKAP [47], RIAD [78], AKAP-Lbc [93], AKAP95 [121], AKAP79 [122].

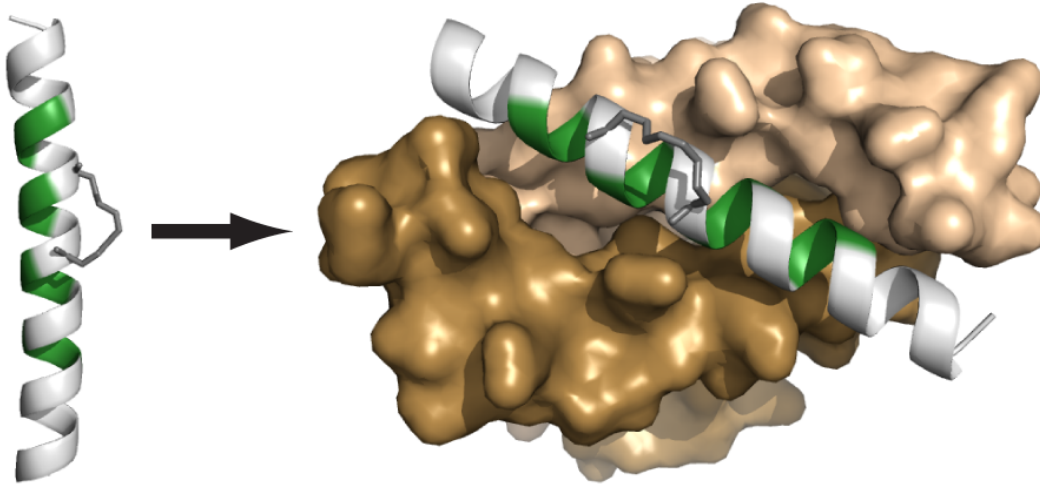


**Figure 3.2 Targeting RI D/D using hydrocarbon stapled peptides.**

Hydrophobic surface of the amphipathic  $\alpha$ -helical peptide is shown in green. The hydrocarbon stapled on the water-exposed surface is shown in dark grey. The right panel shows the stapled peptide binding on the surface of the docking/dimerization (D/D) domain of PKA-RI (wheat and sand) with its hydrophobic surface (green). Structure rendered in PyMol using PDB ID 3IM4 from Sarma et al., 2010.

		<b>RI<math>\alpha</math></b>	<b>RII<math>\alpha</math></b>	
wt:	LEQYANQLADQIIKEATE	22.70	105.90	
v1:		12.05	34.65	
v2:		15.61	11.68	
v3:		1.49	2.57	<b>(STRIAD-1)</b>
v4:		34.12	17.78	
<hr/>				
v1-1:		0.27	5.08	<b>(STRIAD-2)</b>
v1-2:		22.49	245.6	<b>(STRIAD-3)</b>
v1-3:		>1000	48.45	

**Figure 3.3 PKA-R D/D binding of the hydrocarbon stapled peptides.**

Fluorescence polarization was used to determine the dissociation constant (unit: nM) of the peptides and purified protein constructs of the D/D domains from either PKA-R1 $\alpha$  or PKA-R2 $\alpha$ . S5 is represented by asterisk symbol. Final concentration of peptides is 10 nM, and the protein concentration ranges from 0.1 nM to 100  $\mu$ M. Dissociation constants were calculated using nonlinear regression and are presented as mean  $\pm$  standard error of triplicates.

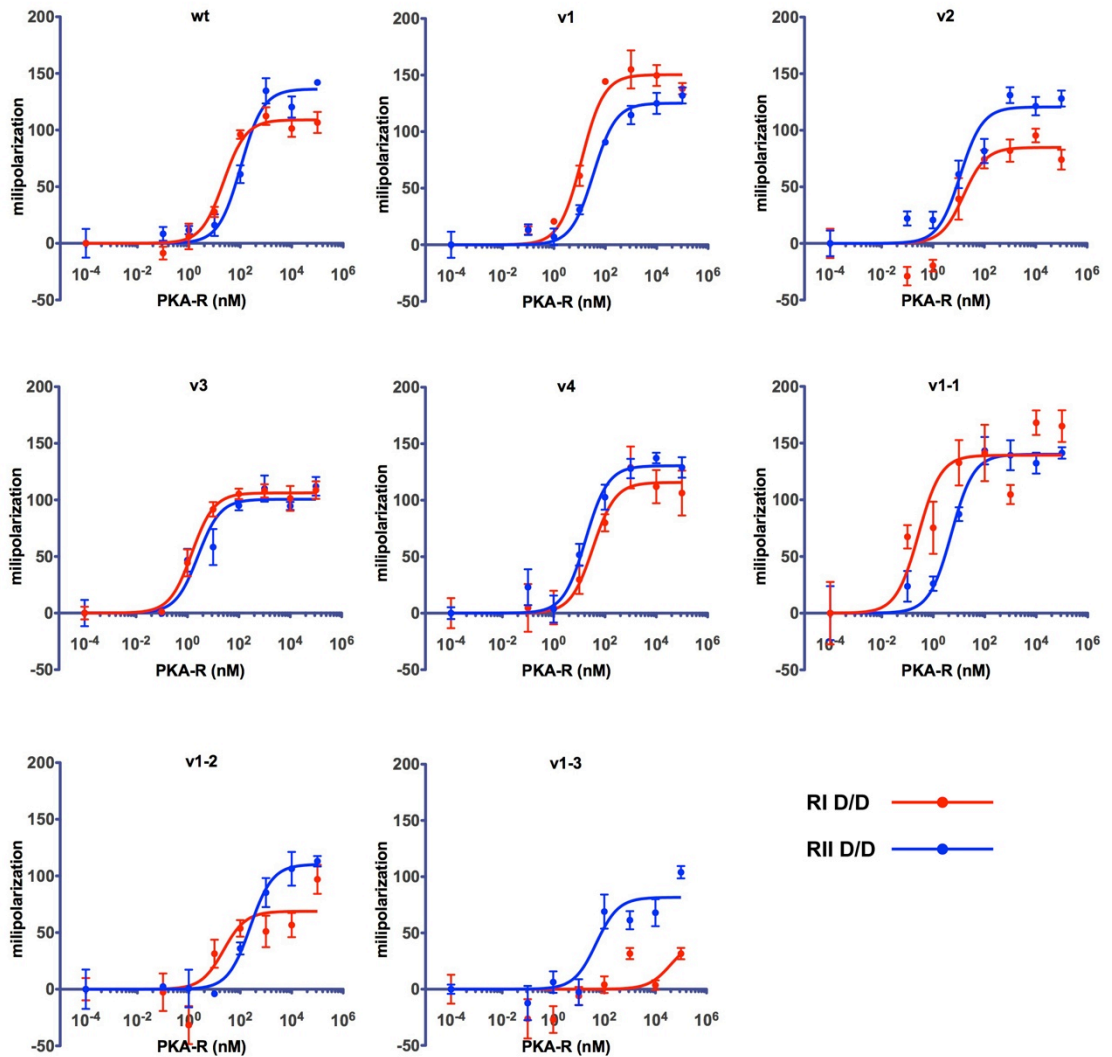


**Figure 3.4 Binding curves of hydrocarbon-stapled peptides on R D/D.**

Fluorescence polarization data of the peptide library in **Table 3.1** were measured using purified protein constructs of the D/D domains from either PKA-R1 $\alpha$  (red) or PKA-R2 $\alpha$  (blue). Peptides were plated at a final concentration of 10 nM and the D/D dimerization domains were tested over a concentration range of 0.1 nM to 100  $\mu$ M. Data was collected in triplicates for each concentration measurement.

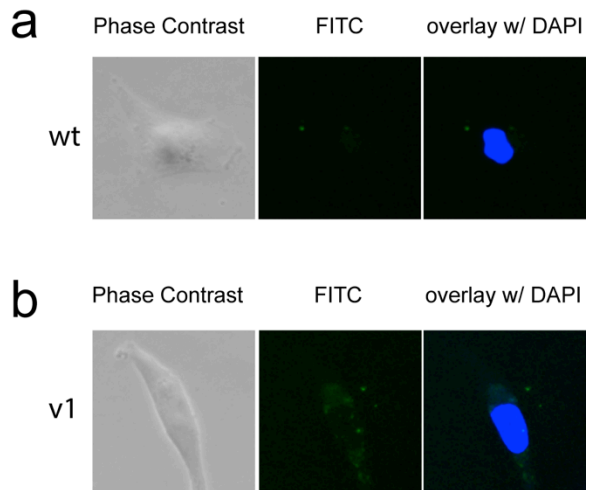


**Figure 3.5 Insufficient uptake of wt and v1.** MDA-MB-231 cells treated with 5  $\mu$ M FITC-labeled wt (a) and v1 (b) for 21 hours. wt did not show apparent uptake. No appreciable uptake for v1 was observed, either. Each image is representative of three replicates.

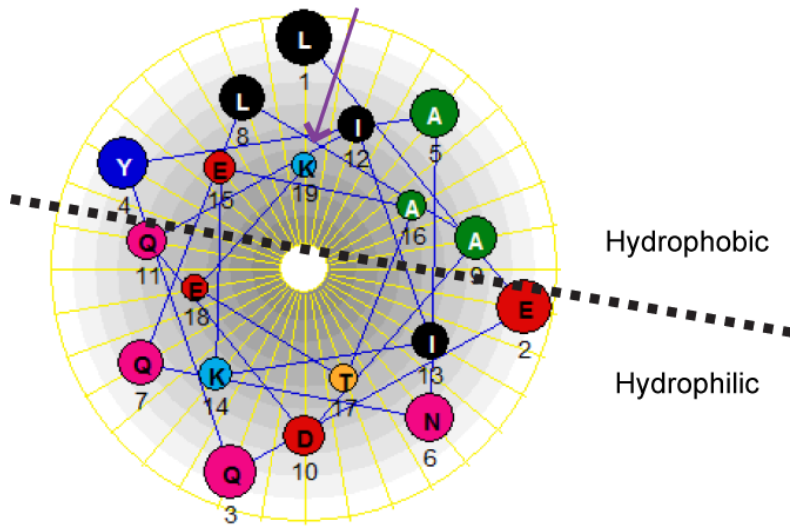


**Figure 3.6 Helical wheel presentation of RIAD sequence.** Hydrophobic and hydrophilic sides of the helix are well defined by its primary amino acid sequence. The additional Lys19 on the C-terminus is pointed out by purple arrow. Picture adapted from DNASTAR.

**Table 3.1  $K_D$  of STRIAD peptides binding full-length R subunits**

Peptide	$K_D$ / [nM] *			
	hRI $\alpha$	hRI $\beta$	hRII $\alpha$	hRII $\beta$
<b>STRIAD-1</b>	5.8 $\pm$ 0.5 (n=6)	14.1 $\pm$ 1.2 (n=4)	19.4 $\pm$ 2.6 (n=6)	166 $\pm$ 41 (n=6)
<b>STRIAD-2</b>	6.2 $\pm$ 0.6 (n=6)	12.1 $\pm$ 2.2 (n=6)	159 $\pm$ 15 (n=6)	492 $\pm$ 41 (n=6)
<b>STRIAD-3</b>	7.3 $\pm$ 0.5 (n=6)	34.5 $\pm$ 2.4 (n=6)	427 $\pm$ 26 (n=6)	649 $\pm$ 52 (n=5)

\* $K_D$  is shown as mean  $\pm$  SEM for replicates of each FP experiment.

The number of replicates is indicated by “n”.

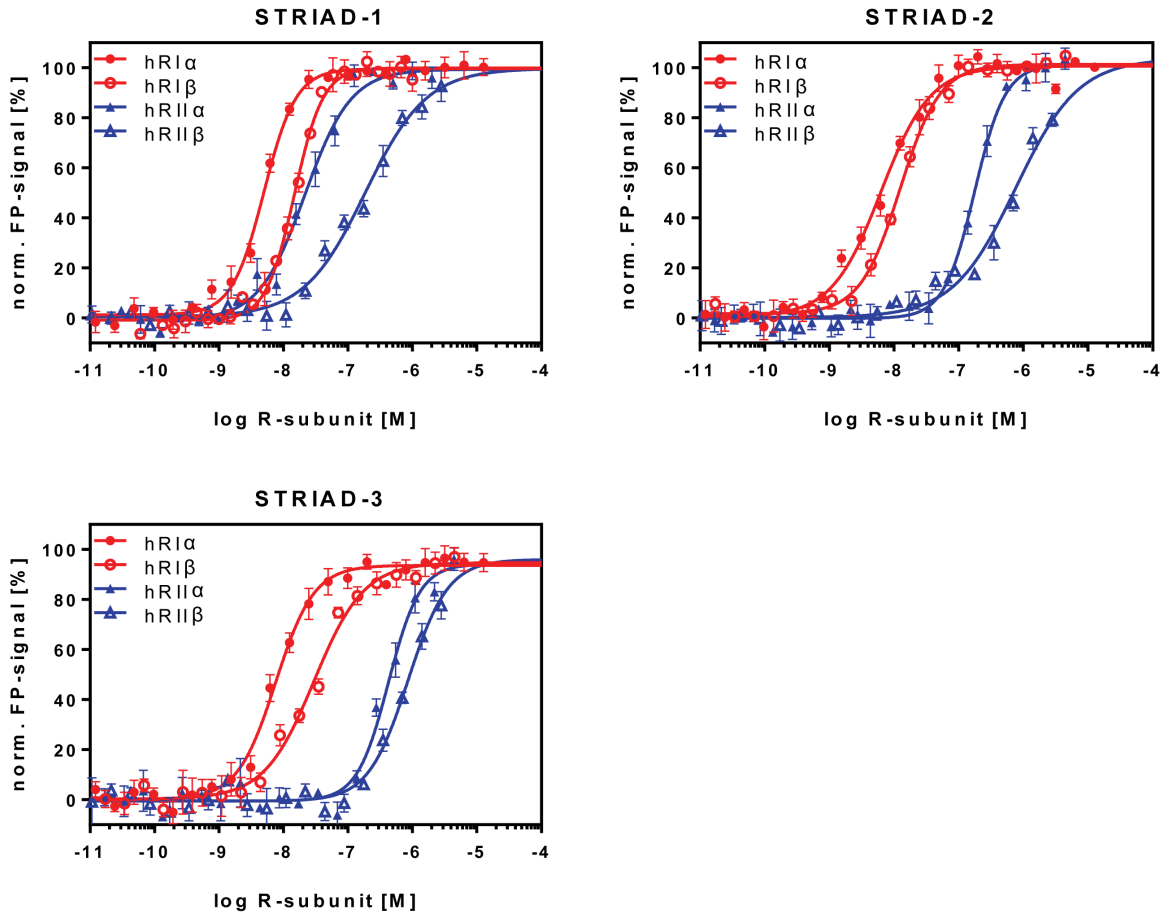


**Figure 3.7 Binding curves of STRIAD peptides on full-length R subunits.**

Normalized fluorescence polarization plotting for data in **Table 3.1** are shown for each of the full-length PKA R subunit isoforms. Peptides were plated at a final concentration of 4 nM and the PKA R-subunits were tested over a concentration range of 60 pM to 10  $\mu$ M PKA-RI is represented in red (closed circles =  $\alpha$ , open circles =  $\beta$ ), and PKA-RII is shown in blue (closed triangles =  $\alpha$ , open triangles =  $\beta$ ).

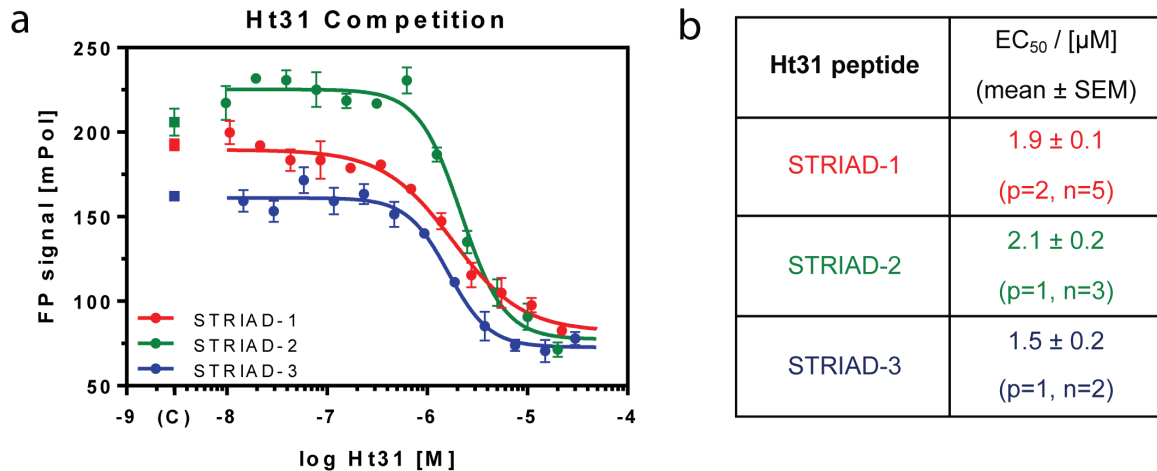


**Figure 3.8 Ht31 competition assay.** (a) FP data are shown for the PKA R-subunit isoform RI $\alpha$  with the three indicated STRIAD peptides. The assay was performed with a final concentration of 4 nM STRIAD and 5 nM of the PKA R-subunits. The competitive peptide Ht31 was tested over a concentration range of 15 nM to 30  $\mu$ M. (b) Apparent EC<sub>50</sub> values of competition assays with RI $\alpha$ . Numbers of replicates were indicated by “n”, numbers of different preparation batches were indicated by “p”.

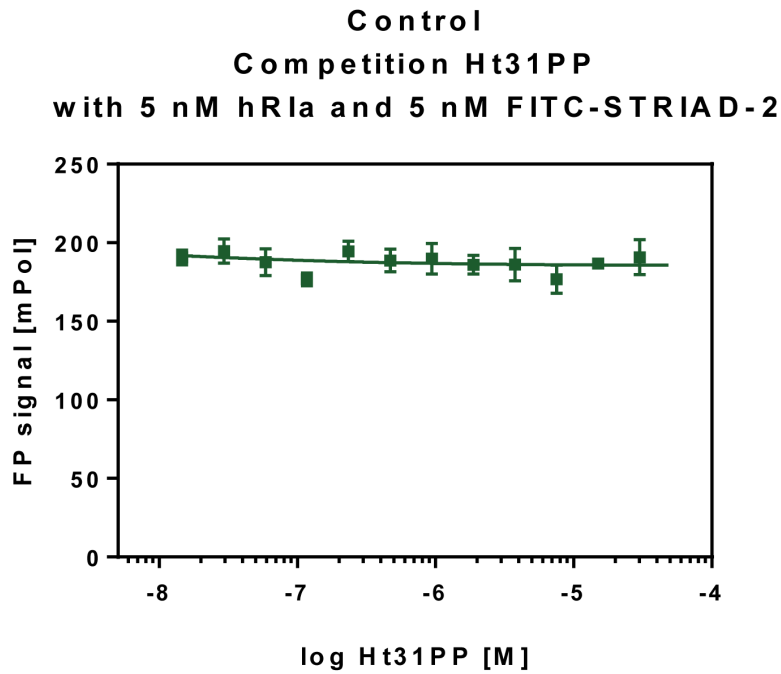


**Figure 3.9 Ht31PP competition assay as control.** FP using a negative control peptide of Ht31 (Ht31PP) was measured with R1 $\alpha$  and STRIAD-2 peptide. Ht31PP is not able to out-compete STRIAD-2 from binding to PKA R1 $\alpha$ .

## MDA-MB-231

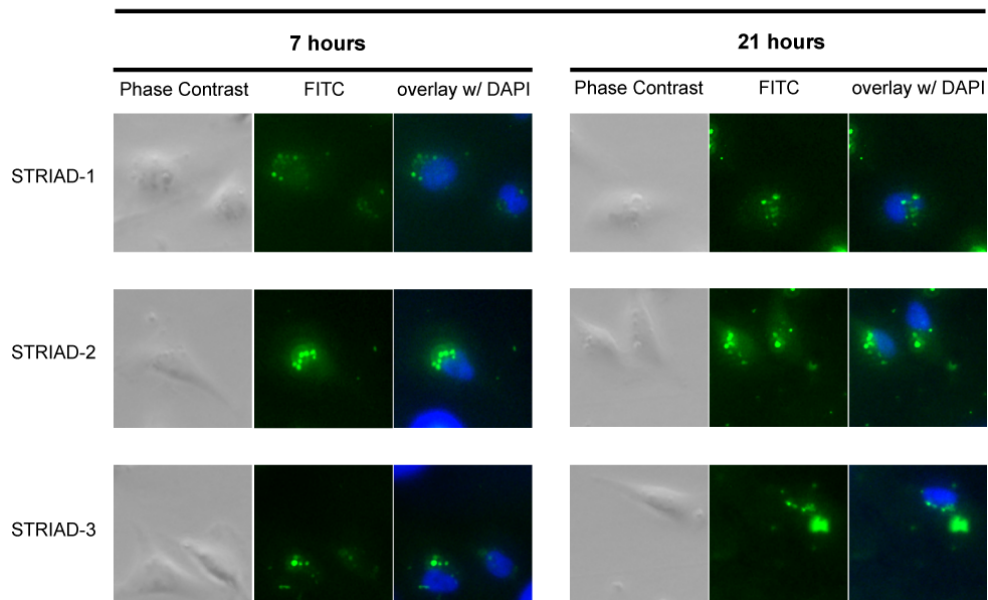


**Figure 3.10** Effective uptake of STRIAD peptides by MDA-MB-231 cells.

Fluorescent images of MDA-MB-231 cells after treatment with FITC-labeled peptides (5  $\mu$ M) for 7 h or 21 h showing that STRIAD-1 -2, and -3 are cell-permeable. Each image is representative of three replicates.

## PC-3

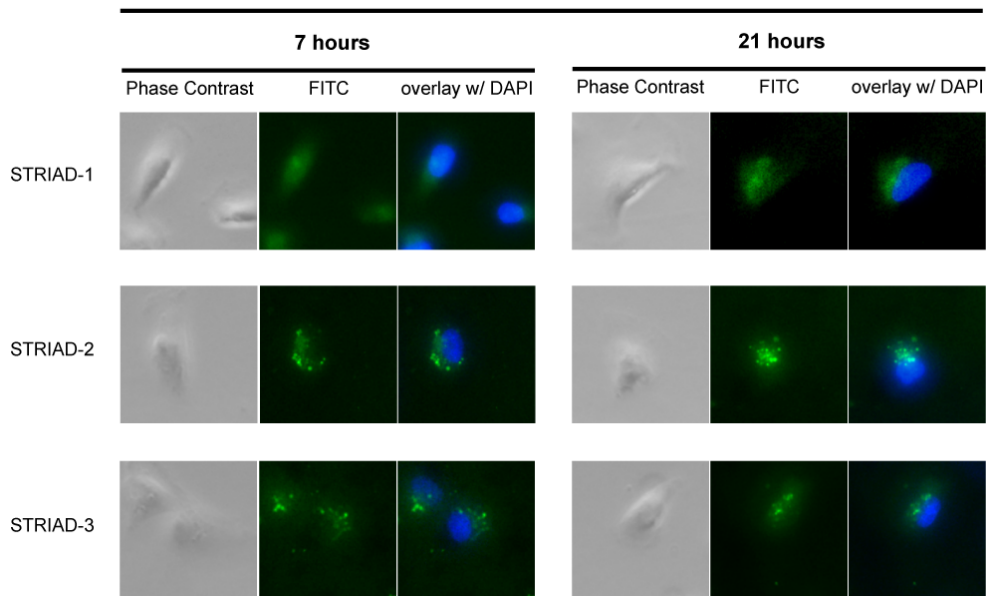


**Figure 3.11 Effective uptake of STRIAD peptides by PC-3 cells.** Fluorescent images of PC-3 cells after treatment with FITC-labeled peptides (5  $\mu$ M) for 7 h or 21 h showing that STRIAD-1 -2, and -3 are cell-permeable. Each image is representative of three replicates.

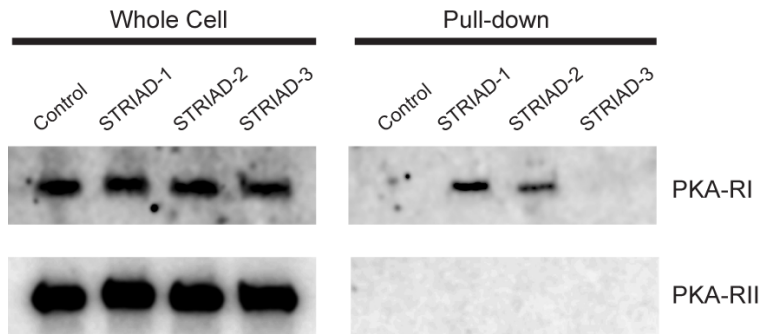


**Figure 3.12 STRIAD peptides selectively target RI in cells.** STRIAD-1 and STRIAD-2 co-precipitate with RI but not RII. MDA-MB-231 cell were treated with 5  $\mu$ M N-terminal biotin-labeled peptides for 12 h. Lysates were pulled down by incubation with avidin-coated resin, and then detected by immunoblotting using PKA-RI and PKA-RII antibodies.

## CHAPTER 4

### SUMMARY

The overall goal of this thesis was to develop chemically engineered helical peptides that intervene in the interaction interface between AKAPs and PKA in an isoform-selective manner. Such peptides, by mimicking endogenous AKAP in cells, can be used to probe type I or type II PKA-regulated signaling and function in a variety of cellular, physiological and pathological models.

We adopted an all-hydrocarbon staple as a helix-stabilizing strategy to chemically modify existing AKB sequences of native or artificial AKAPs. A panel of stapled peptides was derived from each parent sequence, generating a library of peptide candidates based on several different parent sequences. An *in vitro* binding assay called fluorescence polarization (FP) was used to test the library of candidates, selecting out those with high binding affinity and specificity to either the PKA-RI or RII subunit. Several candidates were further examined by a series of cell-based experiments, validating their cellular permeability and ability to target RI or RII in cells. Some parent sequences were further subjected to lysine substitutions and PEG conjugations in order to achieve optimal aqueous solubility and cellular permeability. Using this method, two peptide disruptors that can selectively block RI- or RII-mediated signaling in cells were successfully developed (STAD-2 in **Chapter 2** and STRIAD-2 in **Chapter 3**).

To date, the exact function of AKAP-localized PKA signaling and their mechanism(s) of regulation through RI and RII is largely unclear. This knowledge gap needs to be filled urgently as an increasing number of studies have associated AKAP-mediated signaling complexes with a variety of different diseases. More importantly, the differential roles of RI and RII in physiological and pathological conditions are underscored by multiple studies. This thesis provides valuable chemical biology tools to probe the function of AKAP-mediated PKA activity in an isoform-specific manner, which can be applied in the study of various disease models. For example, combined with proteomics, STRIAD-2 or STAD-2 can be used to identify the primary substrates of type I and type II PKA signaling in normal and disease-state cells. This will be a starting point that enables further biochemical characterization of AKAP-mediated signaling complexes and will ultimately aid in the understanding of how type I and type II PKA-regulated signaling events are involved in carcinogenesis and other diseases. These peptide disruptors also represent a new concept for targeting intracellular protein-protein interactions and displacing functional enzymes while leaving the essential catalytic kinase activity unaffected. This strategy will circumvent the potential for some side effects and will have decreased toxicity and therefore are invaluable tools for discovering novel therapeutic agents to target AKAP-related diseases.

## REFERENCES

1. Coghlan, V.M., et al., *A-kinase anchoring proteins: a key to selective activation of cAMP-responsive events?* Mol Cell Biochem, 1993. **128**: p. 309-19.
2. Johnson, D.A., et al., *Dynamics of cAMP-dependent protein kinase.* Chem Rev, 2001. **101**(8): p. 2243-70.
3. Doskeland, S.O. and D. Ogreid, *Binding proteins for cyclic AMP in mammalian tissues.* 1981.
4. Showers, M.O. and R.A. Maurer, *A cloned bovine cDNA encodes an alternate form of the catalytic subunit of cAMP-dependent protein kinase.* J Biol Chem, 1986. **261**(35): p. 16288-91.
5. Taylor, S.S., et al., *Dynamics of signaling by PKA.* Biochim Biophys Acta, 2005. **30**: p. 1-2.
6. Taylor, S.S., J.A. Buechler, and W. Yonemoto, *cAMP-dependent protein kinase: framework for a diverse family of regulatory enzymes.* Annu Rev Biochem, 1990. **59**: p. 971-1005.
7. Taylor, S.S., et al., *CAMP-dependent protein kinase: prototype for a family of enzymes.* FASEB J, 1988. **2**(11): p. 2677-85.
8. Rosen, O.M. and J. Erlichman, *Reversible autophosphorylation of a cyclic 3':5'-AMP-dependent protein kinase from bovine cardiac muscle.* J Biol Chem, 1975. **250**(19): p. 7788-94.
9. Titani, K., et al., *Amino acid sequence of the regulatory subunit of bovine type I adenosine cyclic 3',5'-phosphate dependent protein kinase.* Biochemistry, 1984. **23**(18): p. 4193-9.

10. Rangel-Aldao, R. and O.M. Rosen, *Effect of cAMP and ATP on the reassociation of phosphorylated and nonphosphorylated subunits of the cAMP-dependent protein kinase from bovine cardiac muscle*. J Biol Chem, 1977. **252**(20): p. 7140-5.
11. Taylor, S.S., et al., *PKA: a portrait of protein kinase dynamics*. Biochim Biophys Acta, 2004. **11**: p. 1-2.
12. Banky, P., et al., *Related protein-protein interaction modules present drastically different surface topographies despite a conserved helical platform*. J Mol Biol, 2003. **330**(5): p. 1117-29.
13. Newlon, M.G., et al., *A novel mechanism of PKA anchoring revealed by solution structures of anchoring complexes*. EMBO J, 2001. **20**(7): p. 1651-62.
14. Kinderman, F.S., et al., *A dynamic mechanism for AKAP binding to RII isoforms of cAMP-dependent protein kinase*. Mol Cell, 2006. **24**(3): p. 397-408.
15. Sarma, G.N., et al., *Structure of D-AKAP2:PKA RI complex: insights into AKAP specificity and selectivity*. Structure, 2010. **18**(2): p. 155-66.
16. Vigil, D., et al., *Conformational differences among solution structures of the type Ialpha, IIalpha and IIbeta protein kinase A regulatory subunit homodimers: role of the linker regions*. J Mol Biol, 2004. **337**(5): p. 1183-94.
17. Ilouz, R., et al., *Localization and quaternary structure of the PKA RIbeta holoenzyme*. Proc Natl Acad Sci U S A, 2012. **109**(31): p. 12443-8.
18. Vigil, D., et al., *Solution scattering reveals large differences in the global structures of type II protein kinase A isoforms*. J Mol Biol, 2006. **357**(3): p. 880-9.
19. Kim, C., et al., *PKA-I holoenzyme structure reveals a mechanism for cAMP-dependent activation*. Cell, 2007. **130**(6): p. 1032-43.

20. Kim, C., N.H. Xuong, and S.S. Taylor, *Crystal structure of a complex between the catalytic and regulatory (R1alpha) subunits of PKA*. Science, 2005. **307**(5710): p. 690-6.
21. Boettcher, A.J., et al., *Realizing the allosteric potential of the tetrameric protein kinase A R1alpha holoenzyme*. Structure, 2011. **19**(2): p. 265-76.
22. Wu, J., et al., *PKA type IIalpha holoenzyme reveals a combinatorial strategy for isoform diversity*. Science, 2007. **318**(5848): p. 274-9.
23. Madhusudan, et al., *Crystal structure of a transition state mimic of the catalytic subunit of cAMP-dependent protein kinase*. Nat Struct Biol, 2002. **9**(4): p. 273-7.
24. Brown, S.H., et al., *Novel isoform-specific interfaces revealed by PKA RIIbeta holoenzyme structures*. J Mol Biol, 2009. **393**(5): p. 1070-82.
25. Zhang, P., et al., *Structure and allostery of the PKA RIIbeta tetrameric holoenzyme*. Science, 2012. **335**(6069): p. 712-6.
26. Brown, S.H., et al., *Implementing fluorescence anisotropy screening and crystallographic analysis to define PKA isoform-selective activation by cAMP analogs*. ACS Chem Biol, 2013. **8**(10): p. 2164-72.
27. Corbin, J.D., S.L. Keely, and C.R. Park, *The distribution and dissociation of cyclic adenosine 3':5'-monophosphate-dependent protein kinases in adipose, cardiac, and other tissues*. J Biol Chem, 1975. **250**(1): p. 218-25.
28. Robinson-White, A. and C.A. Stratakis, *Protein kinase A signaling: "cross-talk" with other pathways in endocrine cells*. Ann N Y Acad Sci, 2002. **968**: p. 256-70.
29. Lohmann, S.M. and U. Walter, *Regulation of the cellular and subcellular concentrations and distribution of cyclic nucleotide-dependent protein kinases*. Adv Cyclic Nucleotide Protein Phosphorylation Res, 1984. **18**: p. 63-117.

30. Carnegie, G.K., C.K. Means, and J.D. Scott, *A-kinase anchoring proteins: from protein complexes to physiology and disease*. IUBMB Life, 2009. **61**(4): p. 394-406.
31. Amieux, P.S. and G.S. McKnight, *The essential role of RI alpha in the maintenance of regulated PKA activity*. Ann N Y Acad Sci, 2002. **968**: p. 75-95.
32. Uhler, M.D. and G.S. McKnight, *Expression of cDNAs for two isoforms of the catalytic subunit of cAMP-dependent protein kinase*. J Biol Chem, 1987. **262**(31): p. 15202-7.
33. Otten, A.D. and G.S. McKnight, *Overexpression of the type II regulatory subunit of the cAMP-dependent protein kinase eliminates the type I holoenzyme in mouse cells*. J Biol Chem, 1989. **264**(34): p. 20255-60.
34. Brandon, E.P., et al., *Hippocampal long-term depression and depotentiation are defective in mice carrying a targeted disruption of the gene encoding the RI beta subunit of cAMP-dependent protein kinase*. Proc Natl Acad Sci U S A, 1995. **92**(19): p. 8851-5.
35. Cadd, G.G., M.D. Uhler, and G.S. McKnight, *Holoenzymes of cAMP-dependent protein kinase containing the neural form of type I regulatory subunit have an increased sensitivity to cyclic nucleotides*. J Biol Chem, 1990. **265**(32): p. 19502-6.
36. Burton, K.A., et al., *Type II regulatory subunits are not required for the anchoring-dependent modulation of Ca<sup>2+</sup> channel activity by cAMP-dependent protein kinase*. Proc Natl Acad Sci U S A, 1997. **94**(20): p. 11067-72.
37. Burton, K.A., et al., *Deletion of type IIalpha regulatory subunit delocalizes protein kinase A in mouse sperm without affecting motility or fertilization*. J Biol Chem, 1999. **274**(34): p. 24131-6.
38. Cummings, D.E., et al., *Genetically lean mice result from targeted disruption of the RII beta subunit of protein kinase A*. Nature, 1996. **382**(6592): p. 622-6.

39. Amieux, P.S., *R1alpha is an essential regulator of protein kinase A in the adult and developing mouse*. 1997.
40. Imaizumi-Scherrer, T., et al., *Accumulation in fetal muscle and localization to the neuromuscular junction of cAMP-dependent protein kinase A regulatory and catalytic subunits R1 alpha and C alpha*. J Cell Biol, 1996. **134**(5): p. 1241-54.
41. Skalhegg, B.S., et al., *Location of cAMP-dependent protein kinase type I with the TCR-CD3 complex*. Science, 1994. **263**(5143): p. 84-7.
42. Kirschner, L.S., et al., *Mutations of the gene encoding the protein kinase A type I-alpha regulatory subunit in patients with the Carney complex*. Nat Genet, 2000. **26**(1): p. 89-92.
43. Jarnaess, E. and K. Tasken, *Spatiotemporal control of cAMP signalling processes by anchored signalling complexes*. Biochem Soc Trans, 2007. **35**(Pt 5): p. 931-7.
44. Wong, W. and J.D. Scott, *AKAP signalling complexes: focal points in space and time*. Nat Rev Mol Cell Biol, 2004. **5**(12): p. 959-70.
45. Burns-Hamuro, L.L., et al., *Distinct interaction modes of an AKAP bound to two regulatory subunit isoforms of protein kinase A revealed by amide hydrogen/deuterium exchange*. Protein Sci, 2005. **14**(12): p. 2982-92.
46. Kovanich, D., et al., *Sphingosine kinase interacting protein is an A-kinase anchoring protein specific for type I cAMP-dependent protein kinase*. Chembiochem, 2010. **11**(7): p. 963-71.
47. Burgers, P.P., et al., *A Small Novel A-Kinase Anchoring Protein (AKAP) That Localizes Specifically Protein Kinase A-Regulatory Subunit I (PKA-R1) to the Plasma Membrane*. J Biol Chem, 2012. **31**: p. 31.
48. Carr, D.W., et al., *Interaction of the regulatory subunit (R1I) of cAMP-dependent protein kinase with R1I-anchoring proteins occurs through an amphipathic helix binding motif*. J Biol Chem, 1991. **266**(22): p. 14188-92.

49. Obar, R.A., et al., *The RII subunit of cAMP-dependent protein kinase binds to a common amino-terminal domain in microtubule-associated proteins 2A, 2B, and 2C*. *Neuron*, 1989. **3**(5): p. 639-45.
50. Colledge, M. and J.D. Scott, *AKAPs: from structure to function*. *Trends Cell Biol*, 1999. **9**(6): p. 216-21.
51. Gold, M.G., et al., *Molecular basis of AKAP specificity for PKA regulatory subunits*. *Mol Cell*, 2006. **24**(3): p. 383-95.
52. Huang, L.J., et al., *Identification of a novel protein kinase A anchoring protein that binds both type I and type II regulatory subunits*. *J Biol Chem*, 1997. **272**(12): p. 8057-64.
53. Angelo, R. and C.S. Rubin, *Molecular characterization of an anchor protein (AKAPCE) that binds the RI subunit (RCE) of type I protein kinase A from *Caenorhabditis elegans**. *J Biol Chem*, 1998. **273**(23): p. 14633-43.
54. Li, H., et al., *Identification, localization, and function in steroidogenesis of PAP7: a peripheral-type benzodiazepine receptor- and PKA (RIalpha)-associated protein*. *Mol Endocrinol*, 2001. **15**(12): p. 2211-28.
55. Banky, P., et al., *Isoform-specific differences between the type Ialpha and IIalpha cyclic AMP-dependent protein kinase anchoring domains revealed by solution NMR*. *J Biol Chem*, 2000. **275**(45): p. 35146-52.
56. Gao, T., et al., *cAMP-dependent regulation of cardiac L-type Ca<sup>2+</sup> channels requires membrane targeting of PKA and phosphorylation of channel subunits*. *Neuron*, 1997. **19**(1): p. 185-96.
57. Kapiloff, M.S., N. Jackson, and N. Airhart, *mAKAP and the ryanodine receptor are part of a multi-component signaling complex on the cardiomyocyte nuclear envelope*. *J Cell Sci*, 2001. **114**(Pt 17): p. 3167-76.
58. Hulme, J.T., et al., *Beta-adrenergic regulation requires direct anchoring of PKA to cardiac CaV1.2 channels via a leucine zipper interaction with A kinase-anchoring protein 15*. *Proc Natl Acad Sci U S A*, 2003. **100**(22): p. 13093-8.

59. Lygren, B., et al., *AKAP complex regulates Ca<sup>2+</sup> re-uptake into heart sarcoplasmic reticulum*. EMBO Rep, 2007. **8**(11): p. 1061-7.
60. Pidoux, G. and K. Tasken, *Specificity and spatial dynamics of protein kinase A signaling organized by A-kinase-anchoring proteins*. J Mol Endocrinol, 2010. **44**(5): p. 271-84.
61. Troger, J., et al., *A-kinase anchoring proteins as potential drug targets*. Br J Pharmacol, 2011. **29**(10): p. 1476-5381.
62. Chen, L., et al., *Mutation of an A-kinase-anchoring protein causes long-QT syndrome*. Proc Natl Acad Sci U S A, 2007. **104**(52): p. 20990-5.
63. Kammerer, S., et al., *Amino acid variant in the kinase binding domain of dual-specific A kinase-anchoring protein 2: a disease susceptibility polymorphism*. Proc Natl Acad Sci U S A, 2003. **100**(7): p. 4066-71.
64. Neumann, S.A., et al., *AKAP10 (I646V) functional polymorphism predicts heart rate and heart rate variability in apparently healthy, middle-aged European-Americans*. Psychophysiology, 2009. **46**(3): p. 466-72.
65. Mauban, J.R., et al., *AKAP-scaffolding proteins and regulation of cardiac physiology*. Physiology (Bethesda), 2009. **24**: p. 78-87.
66. Rawe, V.Y., et al., *WAVE1, an A-kinase anchoring protein, during mammalian spermatogenesis*. Hum Reprod, 2004. **19**(11): p. 2594-604.
67. Luconi, M., et al., *Increased phosphorylation of AKAP by inhibition of phosphatidylinositol 3-kinase enhances human sperm motility through tail recruitment of protein kinase A*. J Cell Sci, 2004. **117**(Pt 7): p. 1235-46.
68. Lin, X., P. Nelson, and I.H. Gelman, *SSeCKS, a major protein kinase C substrate with tumor suppressor activity, regulates G(1)-->S progression by controlling the expression and cellular compartmentalization of cyclin D*. Mol Cell Biol, 2000. **20**(19): p. 7259-72.
69. Wang, M.J., et al., *The Ile646Val (2073A>G) polymorphism in the kinase-binding domain of A-kinase anchoring protein 10 and the risk of colorectal cancer*. Oncology, 2009. **76**(3): p. 199-204.

70. Frank, B., et al., *Association of a common AKAP9 variant with breast cancer risk: a collaborative analysis*. J Natl Cancer Inst, 2008. **100**(6): p. 437-42.
71. Wirtenberger, M., et al., *Association of genetic variants in the Rho guanine nucleotide exchange factor AKAP13 with familial breast cancer*. Carcinogenesis, 2006. **27**(3): p. 593-8.
72. Wirtenberger, M., et al., *The functional genetic variant Ile646Val located in the kinase binding domain of the A-kinase anchoring protein 10 is associated with familial breast cancer*. Carcinogenesis, 2007. **28**(2): p. 423-6.
73. Hundsrucker, C. and E. Klussmann, *Direct AKAP-mediated protein-protein interactions as potential drug targets*. Handb Exp Pharmacol, 2008. **186**: p. 483-503.
74. Verdine, G.L. and G.J. Hilinski, *Stapled peptides for intracellular drug targets*. Methods Enzymol, 2012. **503**: p. 3-33.
75. Alto, N.M., et al., *Bioinformatic design of A-kinase anchoring protein-in silico: a potent and selective peptide antagonist of type II protein kinase A anchoring*. Proc Natl Acad Sci U S A, 2003. **100**(8): p. 4445-50.
76. Burns, L.L., et al., *Isoform specific differences in binding of a dual-specificity A-kinase anchoring protein to type I and type II regulatory subunits of PKA*. Biochemistry, 2003. **42**(19): p. 5754-63.
77. Burns-Hamuro, L.L., et al., *Designing isoform-specific peptide disruptors of protein kinase A localization*. Proc Natl Acad Sci U S A, 2003. **100**(7): p. 4072-7.
78. Carlson, C.R., et al., *Delineation of type I protein kinase A-selective signaling events using an RI anchoring disruptor*. J Biol Chem, 2006. **281**(30): p. 21535-45.
79. Reinton, N., et al., *Localization of a novel human A-kinase-anchoring protein, hAKAP220, during spermatogenesis*. Dev Biol, 2000. **223**(1): p. 194-204.

80. Kim, Y.W., T.N. Grossmann, and G.L. Verdine, *Synthesis of all-hydrocarbon stapled alpha-helical peptides by ring-closing olefin metathesis*. Nat Protoc, 2011. **6**(6): p. 761-71.
81. Lacana, E., et al., *Cloning and characterization of a protein kinase A anchoring protein (AKAP)-related protein that interacts with and regulates sphingosine kinase 1 activity*. J Biol Chem, 2002. **277**(36): p. 32947-53.
82. Taylor, S.S., et al., *Assembly of allosteric macromolecular switches: lessons from PKA*. Nat Rev Mol Cell Biol, 2012. **13**(10): p. 646-58.
83. Taylor, S.S., et al., *PKA: lessons learned after twenty years*. Biochim Biophys Acta, 2013. **1834**(7): p. 1271-8.
84. Welch, E.J., B.W. Jones, and J.D. Scott, *Networking with AKAPs: context-dependent regulation of anchored enzymes*. Mol Interv, 2010. **10**(2): p. 86-97.
85. Herberg, F.W., S.S. Taylor, and W.R. Dostmann, *Active site mutations define the pathway for the cooperative activation of cAMP-dependent protein kinase*. Biochemistry, 1996. **35**(9): p. 2934-42.
86. Skroblin, P., et al., *Mechanisms of protein kinase A anchoring*. Int Rev Cell Mol Biol, 2010. **283**: p. 235-330.
87. Dessauer, C.W., *Adenylyl cyclase--A-kinase anchoring protein complexes: the next dimension in cAMP signaling*. Mol Pharmacol, 2009. **76**(5): p. 935-41.
88. Sanderson, J.L. and M.L. Dell'Acqua, *AKAP signaling complexes in regulation of excitatory synaptic plasticity*. Neuroscientist, 2011. **17**(3): p. 321-36.
89. Diviani, D., et al., *A-kinase anchoring proteins: scaffolding proteins in the heart*. Am J Physiol Heart Circ Physiol, 2011. **301**(5): p. H1742-53.
90. Herberg, F.W., et al., *Analysis of A-kinase anchoring protein (AKAP) interaction with protein kinase A (PKA) regulatory subunits: PKA isoform specificity in AKAP binding*. J Mol Biol, 2000. **298**(2): p. 329-39.

91. Troger, J., et al., *A-kinase anchoring proteins as potential drug targets*. Br J Pharmacol, 2012. **29**(10): p. 1476-5381.
92. Blant, A. and M.P. Czubryt, *Promotion and inhibition of cardiac hypertrophy by A-kinase anchor proteins*. Can J Physiol Pharmacol, 2012. **90**(9): p. 1161-70.
93. Carr, D.W., et al., *Association of the type II cAMP-dependent protein kinase with a human thyroid RII-anchoring protein. Cloning and characterization of the RII-binding domain*. J Biol Chem, 1992. **267**(19): p. 13376-82.
94. Vijayaraghavan, S., et al., *Protein kinase A-anchoring inhibitor peptides arrest mammalian sperm motility*. J Biol Chem, 1997. **272**(8): p. 4747-52.
95. Nakase, I., et al., *Methodological and cellular aspects that govern the internalization mechanisms of arginine-rich cell-penetrating peptides*. Adv Drug Deliv Rev, 2008. **60**(4-5): p. 598-607.
96. Patel, H.H., et al., *Disruption of protein kinase A localization using a trans-activator of transcription (TAT)-conjugated A-kinase-anchoring peptide reduces cardiac function*. J Biol Chem, 2010. **285**(36): p. 27632-40.
97. Verdine, G.L. and L.D. Walensky, *The challenge of drugging undruggable targets in cancer: lessons learned from targeting BCL-2 family members*. Clin Cancer Res, 2007. **13**(24): p. 7264-70.
98. Schafmeister, C.E., J. Po, and G.L. Verdine, *An All-Hydrocarbon Cross-Linking System for Enhancing the Helicity and Metabolic Stability of Peptides*. Journal of the American Chemical Society, 2000. **122**(24): p. 5891-5892.
99. Blackwell, H.E., et al., *Ring-closing metathesis of olefinic peptides: design, synthesis, and structural characterization of macrocyclic helical peptides*. J. Org. Chem., 2001. **66**: p. 5291-302.
100. Bertinetti, D., et al., *Chemical tools selectively target components of the PKA system*. BMC Chem Biol, 2009. **9**: p. 3.

101. Friedrich, M.W., et al., *Imaging CREB activation in living cells*. J Biol Chem, 2010. **285**(30): p. 23285-95.
102. Depry, C., M.D. Allen, and J. Zhang, *Visualization of PKA activity in plasma membrane microdomains*. Mol Biosyst, 2011. **7**(1): p. 52-8.
103. Bar, H.P. and O. Hechter, *Adenyl cyclase and hormone action. I. Effects of adrenocorticotrophic hormone, glucagon, and epinephrine on the plasma membrane of rat fat cells*. Proc Natl Acad Sci U S A, 1969. **63**(2): p. 350-6.
104. Carnegie, G.K., et al., *AKAP-Lbc nucleates a protein kinase D activation scaffold*. Mol Cell, 2004. **15**(6): p. 889-99.
105. Tasken, K. and E.M. Aandahl, *Localized effects of cAMP mediated by distinct routes of protein kinase A*. Physiol Rev, 2004. **84**(1): p. 137-67.
106. Taylor, S.S., et al., *PKA: Lessons learned after twenty years*. Biochim Biophys Acta, 2013. **7**(8): p. 25.
107. Barradeau, S., et al., *Muscle-regulated expression and determinants for neuromuscular junctional localization of the mouse R1alpha regulatory subunit of cAMP-dependent protein kinase*. Proc Natl Acad Sci U S A, 2001. **98**(9): p. 5037-42.
108. Imaizumi-Scherrer, T., et al., *Type I protein kinase a is localized to interphase microtubules and strongly associated with the mitotic spindle*. Exp Cell Res, 2001. **264**(2): p. 250-65.
109. Baillie, G.S., J.D. Scott, and M.D. Houslay, *Compartmentalisation of phosphodiesterases and protein kinase A: opposites attract*. FEBS Lett, 2005. **579**(15): p. 3264-70.
110. Huang, L.J., et al., *D-AKAP2, a novel protein kinase A anchoring protein with a putative RGS domain*. Proc Natl Acad Sci U S A, 1997. **94**(21): p. 11184-9.
111. Wang, Y., et al., *Isoform-selective disruption of AKAP-localized PKA using hydrocarbon stapled peptides*. ACS Chem Biol, 2014. **9**(3): p. 635-42.

112. Miki, K. and E.M. Eddy, *Single amino acids determine specificity of binding of protein kinase A regulatory subunits by protein kinase A anchoring proteins*. J Biol Chem, 1999. **274**(41): p. 29057-62.
113. Walensky, L.D., et al., *Activation of apoptosis in vivo by a hydrocarbon-stapled BH3 helix*. Science, 2004. **305**(5689): p. 1466-70.
114. Walensky, L.D., et al., *A stapled BID BH3 helix directly binds and activates BAX*. Mol Cell, 2006. **24**(2): p. 199-210.
115. Diviani, D., et al., *Pericentrin anchors protein kinase A at the centrosome through a newly identified RII-binding domain*. Curr Biol, 2000. **10**(7): p. 417-20.
116. Lim, C.J., et al., *Alpha4 integrins are type I cAMP-dependent protein kinase-anchoring proteins*. Nat Cell Biol, 2007. **9**(4): p. 415-21.
117. Amieux, P.S., et al., *Compensatory regulation of R1alpha protein levels in protein kinase A mutant mice*. J Biol Chem, 1997. **272**(7): p. 3993-8.
118. Cho-Chung, Y.S., et al., *cAMP-dependent protein kinase: role in normal and malignant growth*. 1995.
119. Casey, M., et al., *Mutations in the protein kinase A R1alpha regulatory subunit cause familial cardiac myxomas and Carney complex*. J Clin Invest, 2000. **106**(5): p. R31-8.
120. Tingley, W.G., et al., *Gene-trapped mouse embryonic stem cell-derived cardiac myocytes and human genetics implicate AKAP10 in heart rhythm regulation*. Proc Natl Acad Sci U S A, 2007. **104**(20): p. 8461-6.
121. Eide, T., et al., *Molecular cloning, chromosomal localization, and cell cycle-dependent subcellular distribution of the A-kinase anchoring protein, AKAP95*. Exp Cell Res, 1998. **238**(2): p. 305-16.
122. Carr, D.W., et al., *Localization of the cAMP-dependent protein kinase to the postsynaptic densities by A-kinase anchoring proteins. Characterization of AKAP 79*. J Biol Chem, 1992. **267**(24): p. 16816-23.